Environmental and Earth Sciences Research Journal
Vol. 11, No. 1, March, 2024, pp. 1-19
Journal homepage: http://iieta.org/journals/eesrj

# 2D Hydrodynamic and Eutrophication Modeling in the Shatt Al-Arab River, Basrah, Iraq

Mohammed Jabbar Mawat*, Ahmed Naseh Ahmed Hamdan

Civil Engineering Department, Engineering College, University of Basrah, Basrah 61001, Iraq

Corresponding Author Email: mohammed.mawat@uobasrah.edu.iq



https://doi.org/10.18280/eesrj.110101

**Received:** 21 October 2023
**Revised:** 13 November 2023
**Accepted:** 20 November 2023
**Available online:** 31 March 2024

***Keywords:***
*eutrophication, hydrodynamic modeling, HEC-RAS, Shatt Al-Arab River, water quality analysis, Water Quality Analysis Simulation Program*

**ABSTRACT**

In this study, a comprehensive 2D hydrodynamic model, integrating HEC-RAS with the Water Quality Analysis Simulation Program (WASP), was developed to assess the water quality and eutrophication levels of the Shatt Al-Arab River in Basrah, southern Iraq. The Shatt Al-Arab River, as the primary water source for Basrah province, features numerous branches along its course, necessitating a detailed analysis of its water quality dynamics. The focus of this investigation was to simulate the river's behavior through a model encompassing a seven-branch network within Basrah city. Employing the EUTRO module, the model simulated key state variables, namely temperature (T), ammonia ($NH_3$), nitrite/nitrate ($NO_2$/$NO_3$), organic nitrogen (ON), total phosphorus (TP), inorganic phosphorus (IP), phytoplankton (PHYTO), dissolved oxygen (DO), and carbonaceous biochemical oxygen demand (CBOD), over a four-day period. The model's outcomes revealed significant fluctuations in the concentrations of ON, $NH_3$, $NO_3$, organic phosphorus (OP), IP, and CBOD at the Basrah Center site, attributed primarily to point source pollution from the river's main branches. Furthermore, the tidal influences were observed to significantly impact the concentrations of these state variables. Notably, the Shatt Al-Arab River exhibited a mesotrophic state throughout most of its course, indicating a moderate level of productivity. This finding is crucial for understanding the river's ecological status and for guiding effective water management strategies. In-depth analysis of the model's results offers valuable insights into the river's water quality dynamics, highlighting the significant impact of local anthropogenic activities and natural tidal phenomena on nutrient concentrations and overall river health. These findings are instrumental for environmental planning and management in the region, particularly in addressing eutrophication and its associated challenges. The study underscores the need for integrated hydrodynamic and water quality modeling to effectively manage and preserve vital water resources in riverine ecosystems.

## 1. INTRODUCTION

Surface water ecosystems, characterized by their intricate interplay of hydrodynamic, chemical, and biological attributes, encompass a diverse range of elements including water depth, flow velocity, suspended solids, dissolved oxygen, nutrients, and the biotic community inhabiting both pelagic and benthic zones. It has been observed that these ecosystems face numerous challenges, notably due to population growth, suboptimal land use planning, and pollutant influx from agricultural, residential, and industrial sources, which collectively contribute to their vulnerability and degradation [1, 2]. Notably, the introduction of pollutants through agricultural runoff, industrial effluents, and untreated sewage is identified as a primary cause of water body contamination, engendering adverse effects on human health and aquatic life [3, 4]. The role of surface water modeling is pivotal, extending its applications to predicting storm and flood impacts, and deciphering the dynamics of marine ecosystems [5]. Crucially, this modeling underpins the formulation of water management strategies, employing mathematical equations and computational algorithms to simulate water movement and its interactions with various environmental agents, including wind, waves, currents, and tidal forces. The complexity of integrated modeling surpasses that of conventional approaches, with key challenges encompassing data scarcity, bathymetric information, model parameterization, and computational demands [6].

Diverse water flow characteristics profoundly influence the distribution of temperature, nutrients, and dissolved oxygen, along with the dispersion of sediments, pollutants, and algae. The implementation of a hydrodynamic model, as facilitated by HEC-RAS, is essential for enhancing the precision and efficacy of sediment, toxic substance, and eutrophication models. It provides critical data on various facets, including water velocities, circulation patterns, mixing and dispersion phenomena, water temperature, and density stratification. Therefore, a comprehensive understanding of a water system's hydrodynamic characteristics is imperative before delving into investigations of sediment transport, toxicity, and water quality. Developed by the Environmental Protection Agency (EPA), WASP is adept at simulating a wide spectrum of

contaminants and temperatures within multi-dimensional geometries of rivers, estuaries, lakes, and reservoirs. Primarily designed for water quality simulation, WASP's latest iteration facilitates integration with other hydrodynamic models to concurrently model both hydrodynamics and pollutant movement. A notable application was observed when Taipei University of Science and Technology effectively merged WASP with the HEC-RAS hydrodynamic model [7]. Literature reveals WASP's proficiency in modeling transport in rivers, often in conjunction with various hydraulic evaluation tools to simulate water quality through external linkage with hydraulic models for flow data.

Several instances illustrate this integration's efficacy. Wool et al. [8] employed the Environmental Fluid Dynamics Code (EFDC) to examine the complex three-dimensional hydrodynamics of the Neuse River Estuary in North Carolina, USA. Here, WASP was instrumental in predicting nutrient cycling, eutrophication, and DO dynamics. The water quality model was further utilized to evaluate Total Maximum Daily Load (TMDL) scenarios. Despite the absence of chlorophyll, a (chl a) readings exceeding the 40 mg/L threshold from 1998-2000, instances of fish mortality were recorded. Ernst and Owens [9] combined SWAT and WASP to simulate chl a and TP levels in Cedar Creek Reservoir, Texas, influenced by watershed dynamics, nine wastewater treatment plants, and atmospheric loading. An 11-year TP mass balance indicated that the majority (87%) of TP originated from nonpoint sources, with wastewater treatment plants (WWTPs) contributing 7%, sediment flux 3%, and atmospheric deposition 3%. Fan et al. [10] assessed the water quality of a tidal river in northern Taiwan by integrating Qual2K with HEC-RAS. Their findings suggested that HEC-RAS-enhanced Qual2K simulations, accounting for tidal effects, yielded water quality indices aligning closely with the river's monitoring data.

Quijano et al. [11] coupled EFDC with WASP for three-dimensional simulations of hydrodynamics and water quality in the Chicago River during storm events, analyzing the impact of combined sewer overflows for varying storm periods. Defne et al. [12] utilized the Regional Ocean Modeling System (ROMS) in tandem with WASP for a comprehensive water quality analysis in Barnegat Bay, New Jersey, highlighting the potential negative impact on phytoplankton DO production due to reduced total nitrogen (TN) near the estuary's mouth. Chueh et al. [13] explored copper distribution in Taiwan's Erren River by combining SWAT and WASP. The study noted a decrease in aqueous copper concentration due to increased river flow, attributed to climate change-induced heightened precipitation. In a comprehensive review of research focusing on the Shatt Al-Arab River, various methodologies have been employed for modeling its dynamics. Khudair and Eraibi [14] concentrated on assessing the impact of Reverse Osmosis (RO) units on the river's salinity. Hamdan et al. [15] monitored the Arabian Gulf's seawater intrusion into the Shatt Al-Arab River using the one-dimensional transport model of HEC-RAS 5.0.5. Mohammed and Al Chalabi [16] evaluated the river's water suitability for various uses, including drinking and irrigation. Al-Asadi et al. [17] explored the temporal, spatial, and vertical variability of salinity in the transitional zone between the river and the Gulf, highlighting saltwater penetration during 2019-2020.

However, a critical limitation identified in these studies is the lack of reliance on hydrodynamic and water quality models for elucidating pollutant transport and distribution through the solution of governing equations. Additionally, most studies overlooked the main source of river pollution, namely sewage discharged through branches in the center of Basrah. This study addresses these gaps by first integrating a 2D HEC-RAS model with the WASP water quality framework, a combination not previously explored. Secondly, it considers the impact of the main branches in Basrah province, identified as primary pollution sources to the Shatt Al Arab River. The objectives of this study are outlined as follows:

- To describe the water quality of the Shatt Al Arab River and its main branches by applying the eutrophication (EUTRO) model, encompassing state variables such as T, $NH_3$, $NO_2/NO_3$, ON, OP, IP, PHYTO, DO, and CBOD.
- To monitor and analyze a range of physical, chemical, and biological parameters for detecting pollutants, nutrients, and other contaminants that affect water quality and aquatic life.
- To identify and characterize the pollution sources entering the river, with a focus on investigating point sources in the main branches within Basrah Center.
- To apply a calibrated/verified model of the Shatt Al Arab River, developed in a preceding study, for a comprehensive analysis.

## 2. OVERVIEW OF SHATT AL-ARAB RIVER

### 2.1 Geography and importance of Shatt Al Arab River

Tigris and Euphrates Rivers meet near Al-Qurnah district in southern Iraq to form Shatt Al-Arab River (Figure 1). Shatt Al-Arab River length is approximately 192-kilometer, the river flows south-eastwards, passing through Basrah City and then, discharging into the Arabian Gulf [18, 19]. The province's seven creeks which are Jubyla, Muftya, Robat, Khandek, Ashar, Khora, and Saraji are connected to Shatt Al-Arab River and they are affected by the tidal phenomenon. Shatt Al Arab River width changes along its length, from 250-300 meters near the Euphrates-Tigris confluence to 600 meters near Basrah City Center and 2000 meters at the estuary [20]. For the last 95 kilometers of its course (near to Umm Al Rasas Island), the river forms part of the border between Iraq and Iran [21, 22]. In addition to transportation, Shatt Al Arab River has an important role in delivering water for domestic use, irrigation, and manufacturing [23]. Several tributaries of Shatt Al-Arab River, including Al-Sweeb, Ezz, Garmat Ali, Karkheh, and Karun Rivers, discharged into it over its course. Currently, these contributions as well as the low flow rate from Tigris and Euphrates Rivers have been decreased as a result of surrounding governments' policies, which resulted very significant increase in Total Dissolved Solid (TDS) values in Shatt Al Arab River due to the effect of salinity intrusion from the Arabian Gulf [15, 24, 25]. Shatt Al-Arab River has significant importance since it facilitates agricultural productivity within a region characterized by aridity and a hot, humid environment. The water system of Shatt Al Arab River is now under increasing strain, both in terms of water quantity and quality [21].

The change in the hydrological status of the Shatt Al Arab River over the last decade has adversely affected the quality of the river's water. The monthly average concentration of TDS of the Shatt Al-Arab at Basrah Center is plotted in Figure 2. The TDS concentrations of these years reflect the strength of the correlation with the discharges of the river. A convergence

of concentrations was observed over the years 2010 and 2013, less than 2009, due to relative stability of the discharge, while the highest concentrations were recorded in 2018, which was marked by a sharp decrease in discharge.

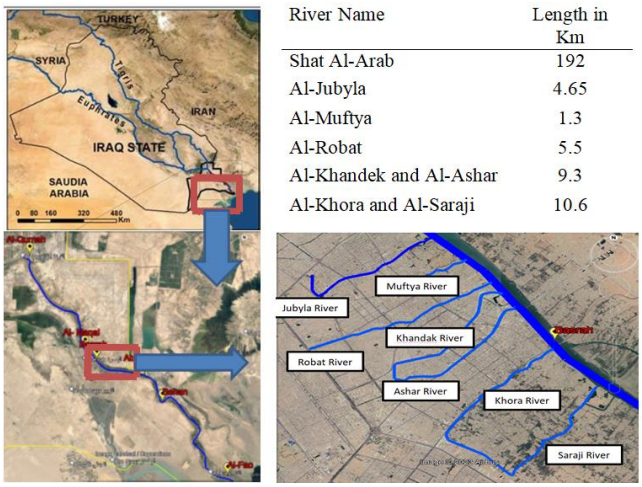


| River Name | Length in Km |
|---|---|
| Shat Al-Arab | 192 |
| Al-Jubyla | 4.65 |
| Al-Muftya | 1.3 |
| Al-Robat | 5.5 |
| Al-Khandek and Al-Ashar | 9.3 |
| Al-Khora and Al-Saraji | 10.6 |

**Figure 1.** Shatt Al Arab River and its main branches

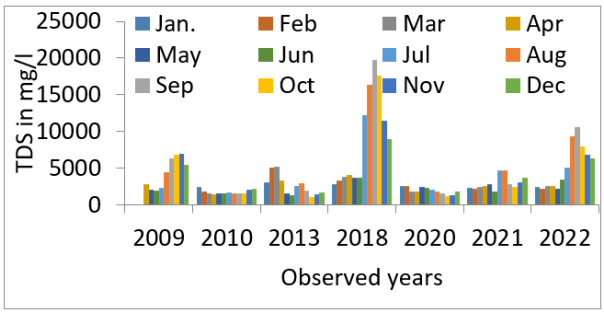


**Figure 2.** The monthly average concentration of the TDS at Basrah Center during different years

### 2.2 Pollution problem in the Shatt Al Arab River

Urban sewage and industrial wastewater are usually discharged directly into the river or its branches through discharge pipes/channels at fixed locations. This type of water pollution is usually called point source pollution, Figure 3. Untreated wastewater contains various pollutants that can contaminate the river and its ecosystems. Wastewater often contains high levels of organic matter, nutrients (such as nitrogen and phosphorus), heavy metals, and other pollutants. When discharged into the river, these substances degrade water quality, leading to decreased oxygen levels and an increase in suspended solids.

### 2.3 Flow data and boundary conditions (BC)

The HEC-RAS model is suitable with a broad range of boundary. Boundary conditions (BC) include external BC along the borders of the 2D area, internal BC such as intake structure, and global BC applied to the whole model such as solar radiation and atmospheric pressure.

There are four external BC types that may be connected to the boundaries of 2D flow area, these are:

- "Flow Hydrograph"
- "Stage Hydrograph"
- "Normal Depth"
- "Rating Curve"

Flow and stage hydrograph BC can be used as upstream and downstream BC. The stage hydrograph may serve as the downstream BC in situations when a stream discharges into a backwater environment, such as an estuary, where the height of the water surface is influenced by tidal oscillations [26].

The BC required to solve the 2D depth averaged equations, Figure 4, are:

- At solid boundaries, the slip BC is applied in HEC-RAS. The velocity component normal to the solid boundary is set to be zero.
- At open boundaries, the stage hydrograph at downstream BC and flow hydrograph at upstream BC is applied by line BC command.

**Figure 3.** Different types of point sources pollutant on the main branches

2.3.1 Upstream BC

Monitoring stations were distributed on the main and secondary rivers contributing to the water supply to Shatt Al-Arab River to record the daily discharge, by official institutions (Directorate of Water Resources, National Center for Ware Resources Management), as shown in Figure 5.

Unfortunately, as can be seen from the figure, there is no discharge monitoring station in Qurnah city, which will be the upstream boundary condition of the model. Therefore, it can be relied on a previous model [27], named assistant model, simulating the same study area, including the impact of the

main rivers extending from Qalat Saleh regulator to the port of Abu Flus. Where, the discharge can be extracted as the results of the model at the confluence in Qurnah city, Figure 6. This method will shorten many and expensive field tests and measurements to calculate the discharge.

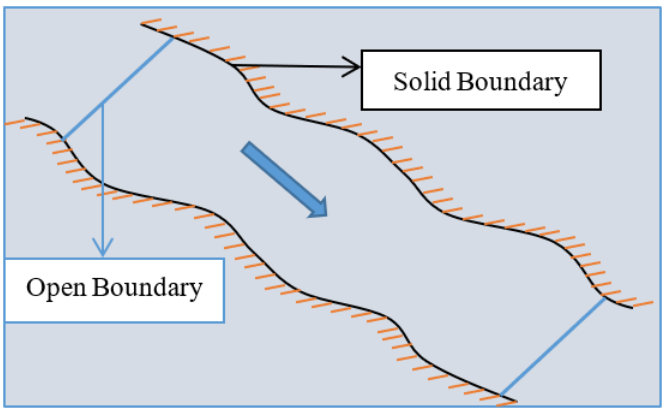


**Figure 4.** The boundary conditions in the model


**Figure 5.** Available flow monitors of the study area

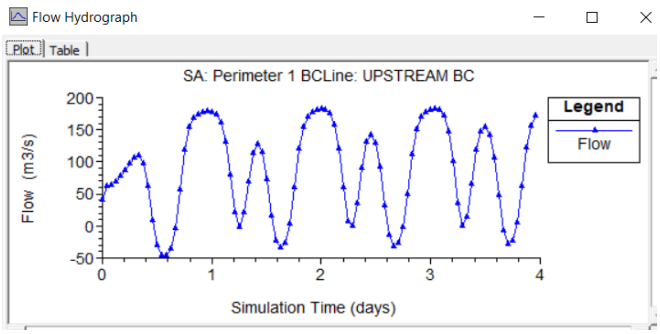


**Figure 6.** Flow hydrograph of assistant model's output used as upstream boundary conditions at the confluence in Qurnah city

2.3.2 Downstream BC

A recorded hourly water stages at Al-Fao station, Figure 7 represents downstream BC.

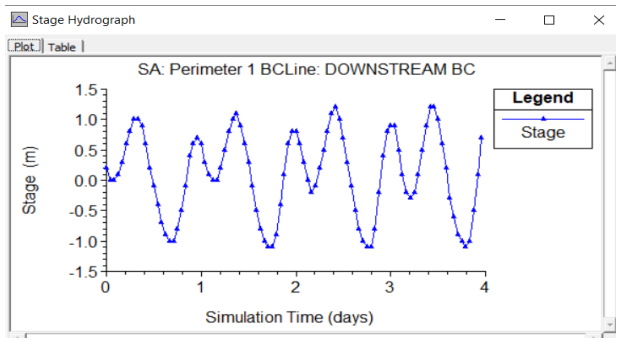


**Figure 7.** Observed water stages for downstream boundary conditions at Al-Fao station

## 3. MATHEMATICAL CONCEPTS

Since fluid and ecological equations are invariably coupled, water quality models are usually characterized by high degrees of complexity and very difficult mathematical problems. The system of equations for a water quality model must consist of at least the balances of mass, momentum, energy and entropy, and the equations describing chemical, biochemical, and biological processes [28]. Hence, the water quality model performance is largely dependent on the description of the circulation given by the hydrodynamic model [29], where the water flow characteristics have significant impact on pollutants transport during either dispersion and advection processes. Therefore, the water quality modeling methodology has been done by using sequentially a three sub models to integrate the comprehensive Shatt Al Arab River modeling: Hydrodynamic model by HEC-RAS, heat model and eutrophication model by WASP. HEC-RAS 2D and WASP External Coupler performed by Python was used in model building. The 2D Shallow-Water equations are listed in the study by Mawat and Hamdan [30]. The corresponding governing equations of water quality (EUTRO) model are listed in the study by Mawat and Hamdan [31].

## 4. SHORT-TERM EUTRO MODEL APPLICATION

Eutrophication is the process in which excessive growth of algae occurs in a water body due to excessive minerals and nutrients. This process may end in oxygen depletion of the water body after the bacterial degradation of the algae. The simulation period was taken as 4 days (23 Aug. to 26 Aug. 2022) and the sampling interval depended on the tidal chart. In other words, the sampling time is at every highest of high water level and lowest of low water level within one day, In order to show the extent of the effect of the tidal phenomenon on the concentrations of pollutants on the one hand, the time interval between the highest tide and the lowest ebb is about 6 hours, which is long enough for chemical reactions for most pollutants on the other hand. Figure 7 represents of a sampling interval during simulation. The comprehensive model of Shatt Al Arab River was run for four days to reproduce EUTRO model of the river. The state variables of this model include T, $NH_3$, $NO_2/NO_3$, ON, TP, IP, PHYTO, DO, and CBOD.

### 4.1 The sites of sampling collection

The largest challenge during the on-site work was the need to take samples from the boundary conditions of the model

simultaneously, as there is a large distance separating the sampling sites, namely the upstream point in Qurnah city, the downstream point in Al-Fao city, and the middle point (for validation) in the center of Basrah City. Accordingly, three groups were formed to cover the mentioned sites, and trained on the correct sampling method, such as the method of fixing oxygen in the required location according to the Winkler method and storage conditions.

The state variables that have been studied and tested on site or in the laboratory which that contribute to the Integrated EUTRO model, namely, T, ON, $NH_3$, $NO_3$, OP, IP, DO, CBOD, and PHYT. Where the samples were collected by using bottles made of polyethylene, except for DO since the Winkler bottles 300 milliliters were used as shown in Figure 8, from depth ranging (15-25) centimeters under the surface of the water. Then it was tightly closed and kept refrigerated by using a Cool Box case filled with crushed ice until returned to the laboratory. Some factors were measured directly in the field and others were treated in the laboratory and the laboratory samples analyzed and conducted in the Marine Science Center and Basrah Sewer Directorate laboratories.

**Figure 8.** Instruments and utilities of the field work

The water temperatures were measured and recorded in situ using a German-made multi-meter model 340i and the output was expressed in Celsius (°C). Iodometric titration (Winkler titration) [32] is a method conducted in the field to prevent any changes in oxygen levels that may occur due to delays in sample collecting and subsequent assessment. For PHYTO in term Chlorophyll-a, one liter of water was taken from each of the study areas in unused, well-sealed polyethylene bottles and put in a refrigerator. When the samples were brought back to the lab, they were filtered using filter paper of type GF/C with 1 millilitre of a saturated solution of magnesium carbonate MgCO3 added to the last 10 milliliters. After the filtration process was finished, the paper was folded and transferred. When measuring, the paper was left at laboratory temperature for a few minutes. It was then ground without exposure to light with a manual glass mortar grinder after adding 4 ml of 90% acetone. The leachate was transferred to the glass tube, and the grinding vessel was rinsed with 4 ml of acetone and added to the glass tube. The volume was then filled to 10 millilitres and kept in the dark at 4°C for 18 hours. The use of acetone 90% as a blank reference, according to the concentration of chlorophyll-a based on Lorenzen's equation, Chlorophyll-a can be calculated [33]. For Nitrogen Forms (ON, $NO_2$, $NO_3$, and $NH_3$), the Total Kjeldahl Nitrogen (TKN) analysis is often performed to get information on the overall nitrogen content present in the given sample.

### 4.2 Point source pollutions

After conducting surveys and research on the branches of the Shatt Al-Arab River, variant major and minor pollution points were recorded, Table 1, and the locations of most effective source were fixed as shown in Figure 9. The discharge and pollutant's concentration of the point source is assumed relatively steady by mean does not vary with time significantly. Therefore, the measurements of state variables were done one time for each point source.

**Table 1.** Characteristics and point source distribution of the main branches

| Branch Name | Pollutant Source Type | Number |
|---|---|---|
| Al-Jubyla | (75-200) mm Dia. | 26 |
| | Pump station outlet | 1 |
| Al-Muftyah | (75-250) mm Dia. | 13 |
| Al-Robat | (75-300) mm Dia. | 57 |
| | Pump station outlet | 4 |
| Al-Khandak and Al-Ashar | (75-400) mm Dia. | 90 |
| | Pump station outlet | 3 |
| Al-Khora and Al-Saraje | (75-200) mm Dia. | 68 |
| | Pump station outlet | 2 |

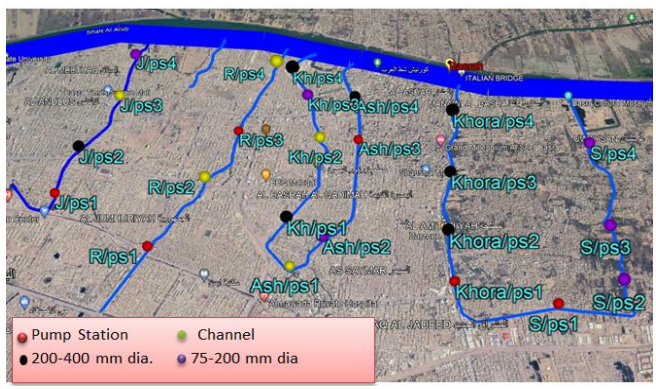


**Figure 9.** The considered point's sources distribution along main branches

## 5. RESULTS AND DISCUSSION

WASP results can be divided into two sections, water temperature results and EUTRO results. Since the temperature affects the rate of chemical reactions that occur in water, such as the breakdown of organic matter. So, the modelling of water temperature distribution was a proactive step of EUTRO modelling.

### 5.1 Water temperature results

The simulation of temperature variation along the river was done during the hot season by applying the boundary conditions of the water temperature at upstream and downstream of the river, Figure 10.

The time series of water temperature variation was plotted at Basrah Center station and compared with observed data, as a validation step, as shown in Figure 11 (a). The results are plotted in Figure 11 (b). The figure showed that the range of temperature was between 32-35°C through a different period during the simulation period. It can be seen from the figure that the calculated value at hour 18. 00 was slightly more than that calculated at hour 10. 00. The maximum difference between the periods was 0.5°C, which can be attributed to the water volume that storages in the segment. Since the WSE at hour 18. 00 is lower. Moreover, the larger and lower range of temperature variation was recorded at Qurnah and Basrah Center stations respectively. The reason for this approach, that the calculated volume of water in Qurnah segment was less than that calculated in Basrah Center, in other words, the shallow region of the river is highly influenced by other parameters such as air temperature. This approach obviously was recognized in the water temperature behaviors of the main branches as shown in Figure 12.

It can be seen that the water temperature of branches strongly affected by the weather conditions, where, the water temperature at time 14. 00 was larger than that recorded at time 08. 00 along the branches except at junctions, the branches meet with the Shatt Al Arab River, where the volume of this segments is large compared with other segments. Also, a validation step was made throughout this figure. A spatial distribution of water temperature at Basrah Center and Fao site was illustrated in Figure 13.

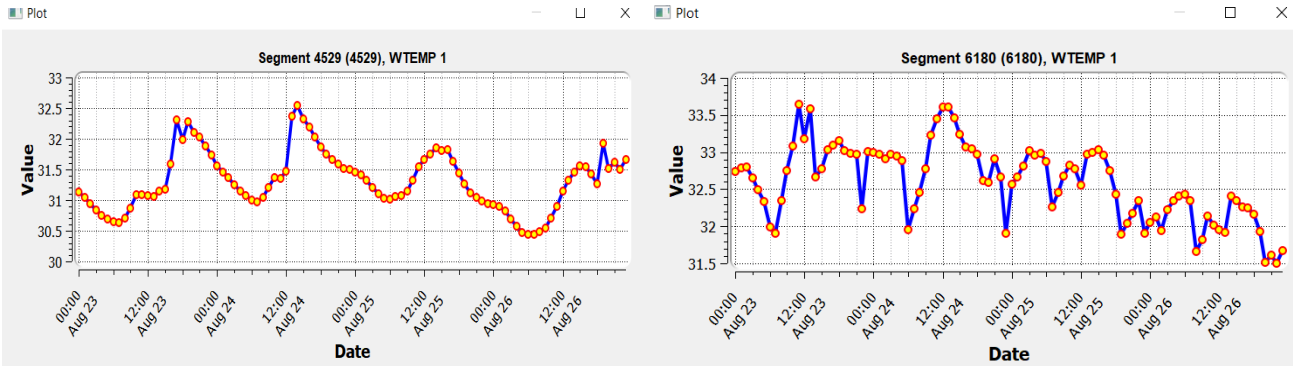


(a) Upstream boundary condition (b) Downstream boundary condition

**Figure 10.** Time series of water temperature

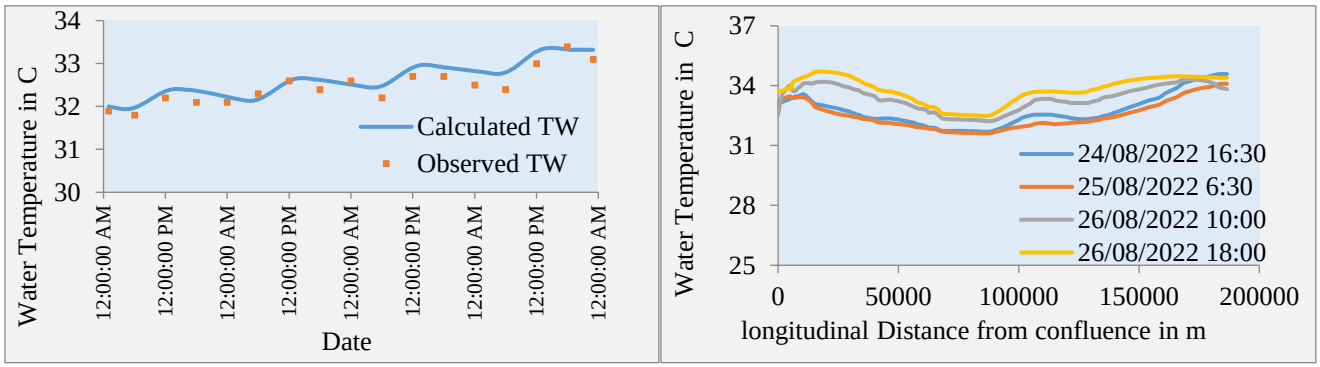


(a) Water temperature variation at Basrah Center station (b) Water temperature variation along the Shatt Al Arab River

**Figure 11.** Water temperature results during simulation time at different time periods

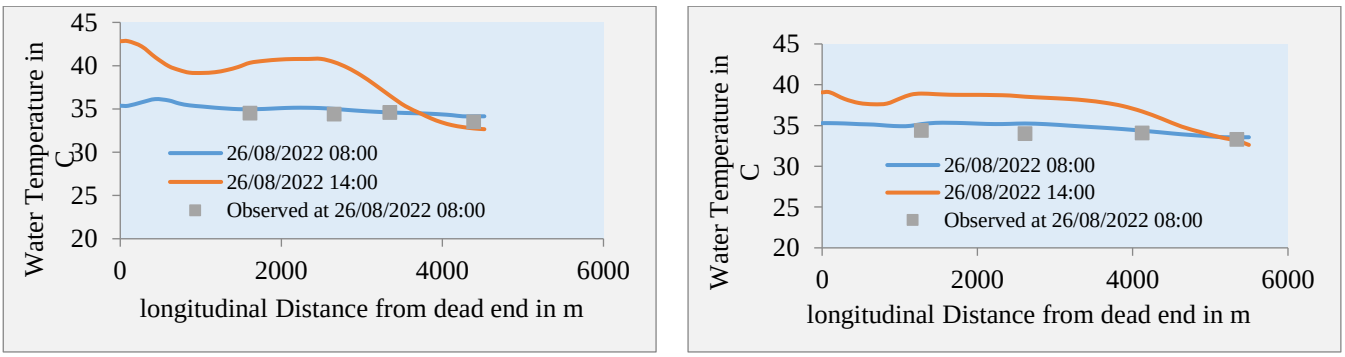


(a) Jubyla River (b) Robat River

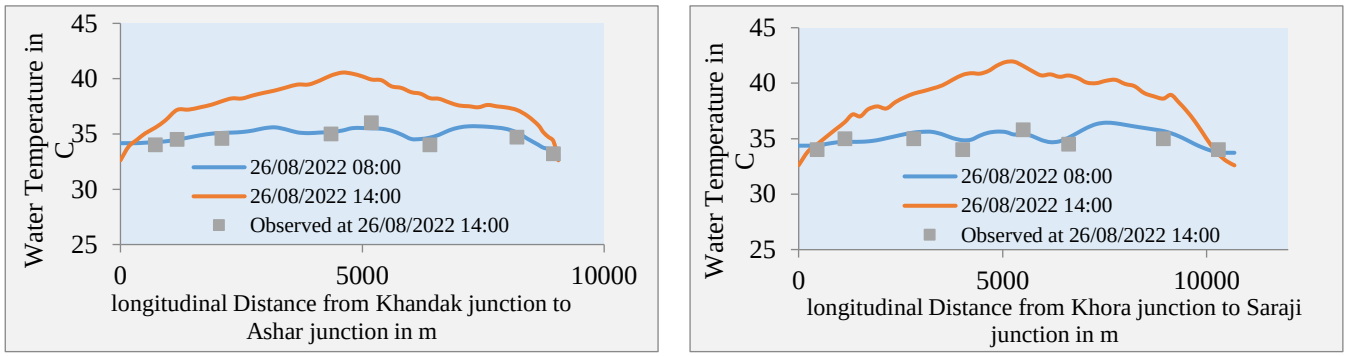


(c) Khandak and Ashar Rivers (d) Khora and Saraji Rivers

**Figure 12.** Water temperature variation along the main branches of the Shatt Al Arab River

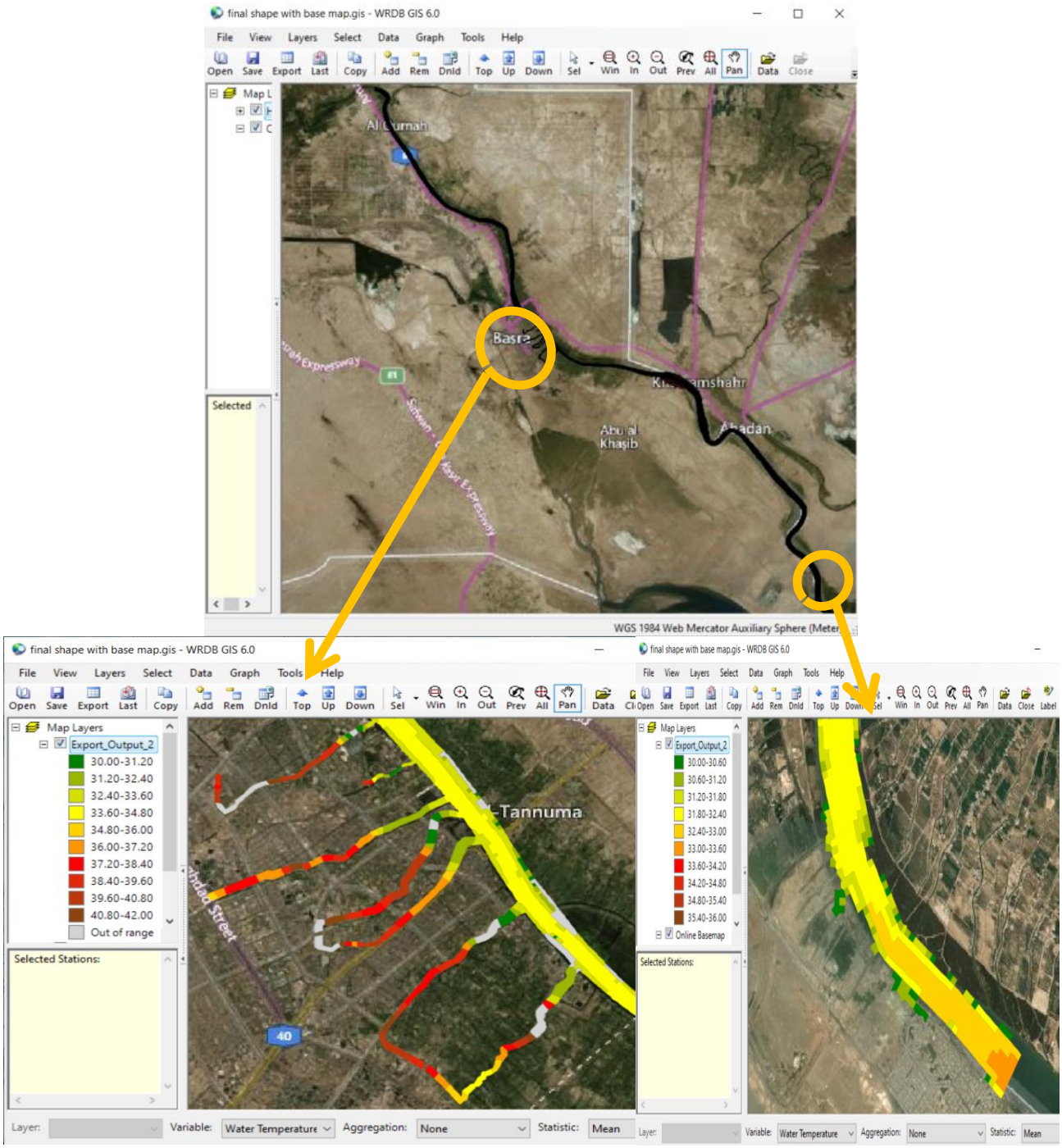


**Figure 13.** Spatial distribution of water temperature at Basrah Center and Fao section

### 5.2 EUTRO results

Eight state variables have been considered during this model as previously mentioned. Accordingly, these variables were divided by type in the following sections.

5.2.1 Nitrogen compounds state variables

ON, $NH_3$, and $NO_3$ state variables are investigated and their results are plotted in Figure 14. The figure tracked the results in consecutive periods, as fixed by legend, during the simulation time. In general, it was observed that there is a harmony between the results explaining the relationship between these compounds. For example, it has been observed that ammonia values decrease with time, while corresponding to an increase in nitrate values, through the nitrification process. While, for ON, the reduction in values was recorded due to the hydrolysis process. The results varied from (1.0 to 0.8), (1.5 to 0.8), and (3.5 to 4.2) mg/l at Basrah Center for ON, $NH_3$, and $NO_3$ respectively.

The corresponding results of these state variables of the main branches were shown in Figures 15-18. All results were calculated at two different periods, High Tide (HT) and Low Tide (LT) according to Basrah Center tide table. It can be concluded from these figures the following.

- During HT, the concentration of ON has been reduced because of the dilution process that occurs through interring additional water volume into the streams which in turn, increase the mineralization process.
- During HT, the concentration of $NH_3$ has been reduced because of the increment of DO level that occurs during HT period which in turn, increase the nitrification process.
- During HT, the concentration of $NO_3$ has been increased because of the increment of DO level that occurs during HT period which in turn, increase the nitrification process.
- The concentrations of Nitrogen compounds state variables were slightly affected by the tide at the far ends of the Rivers from the Shatt Al Arab River because the flow velocity at these dead ends was approximately zero. Colored spatial distributions of the Total Nitrogen (TN) and NH3 system are plotted in Figure 19. As shown in the figure, the main branches have high values compared with the river.

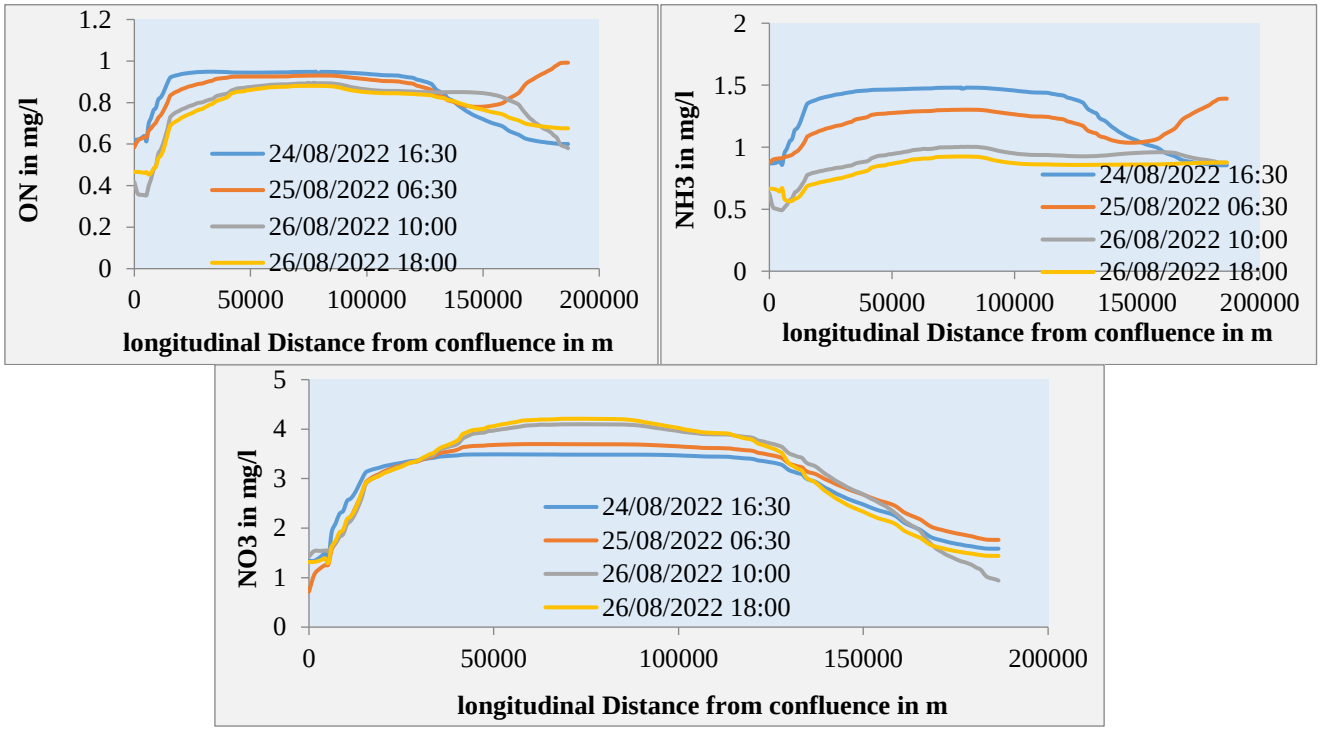


**Figure 14.** ON, $NH_3$, $NO_3$ variation along the Shatt Al Arab River at different periods

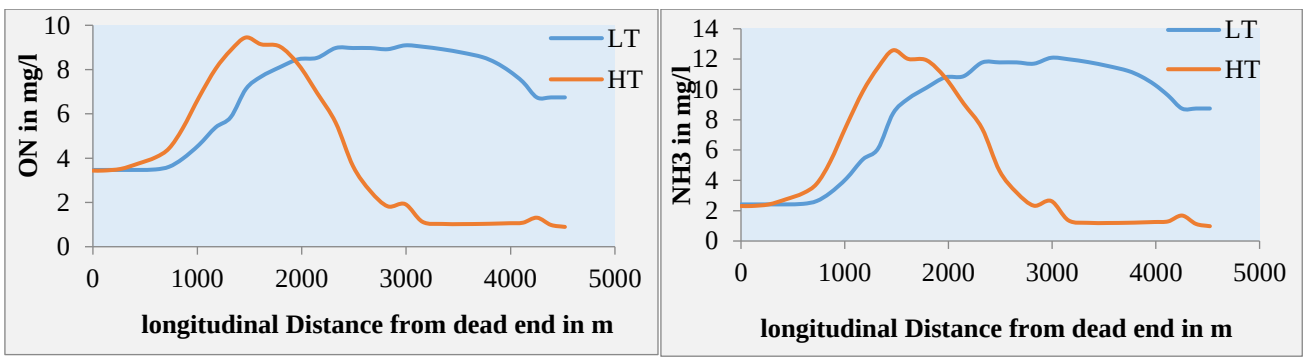

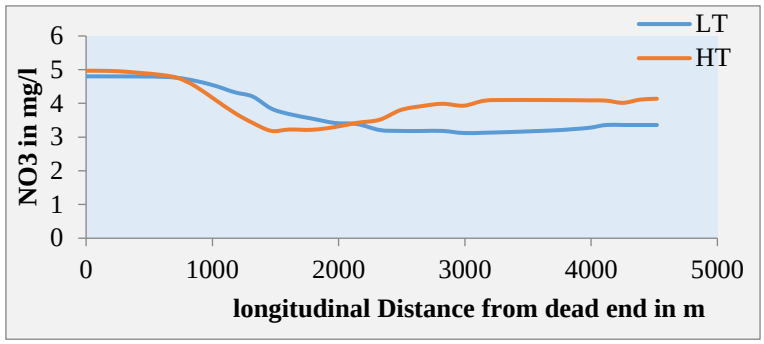


**Figure 15.** State variables of Nitrogen compound for Jubyla River

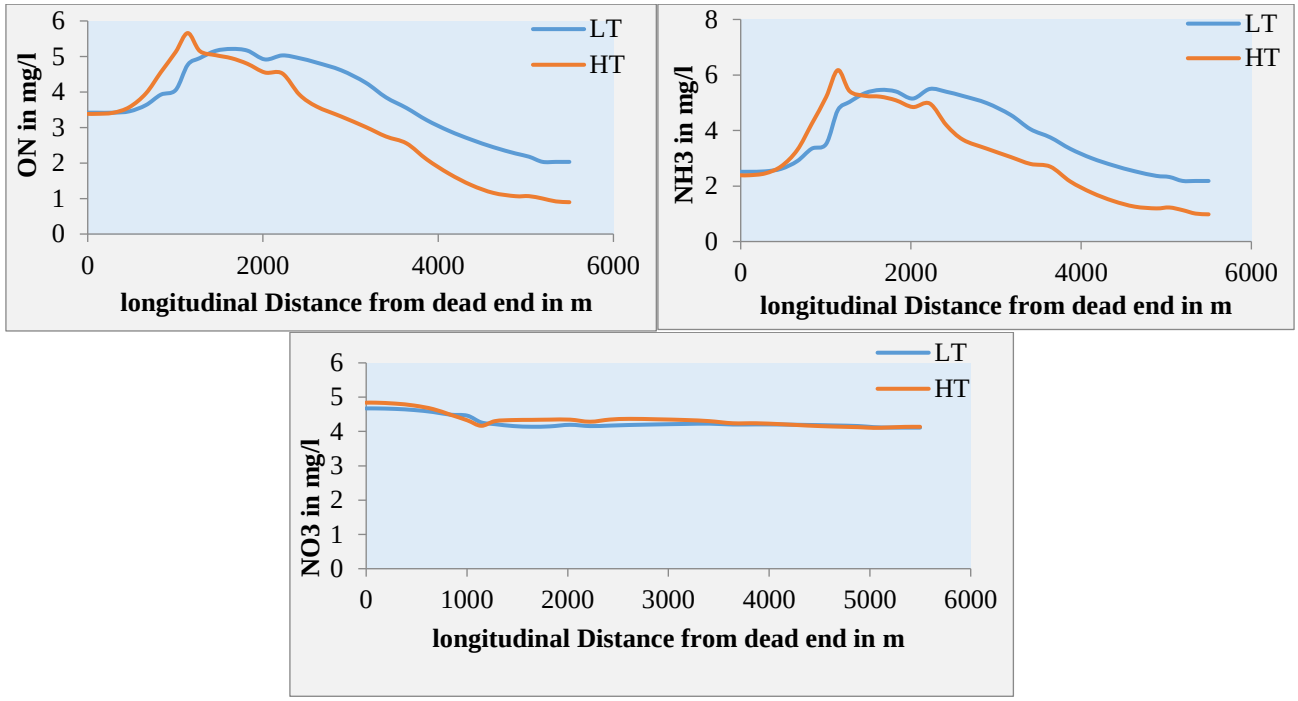


**Figure 16.** State variables of Nitrogen compound for Robat River

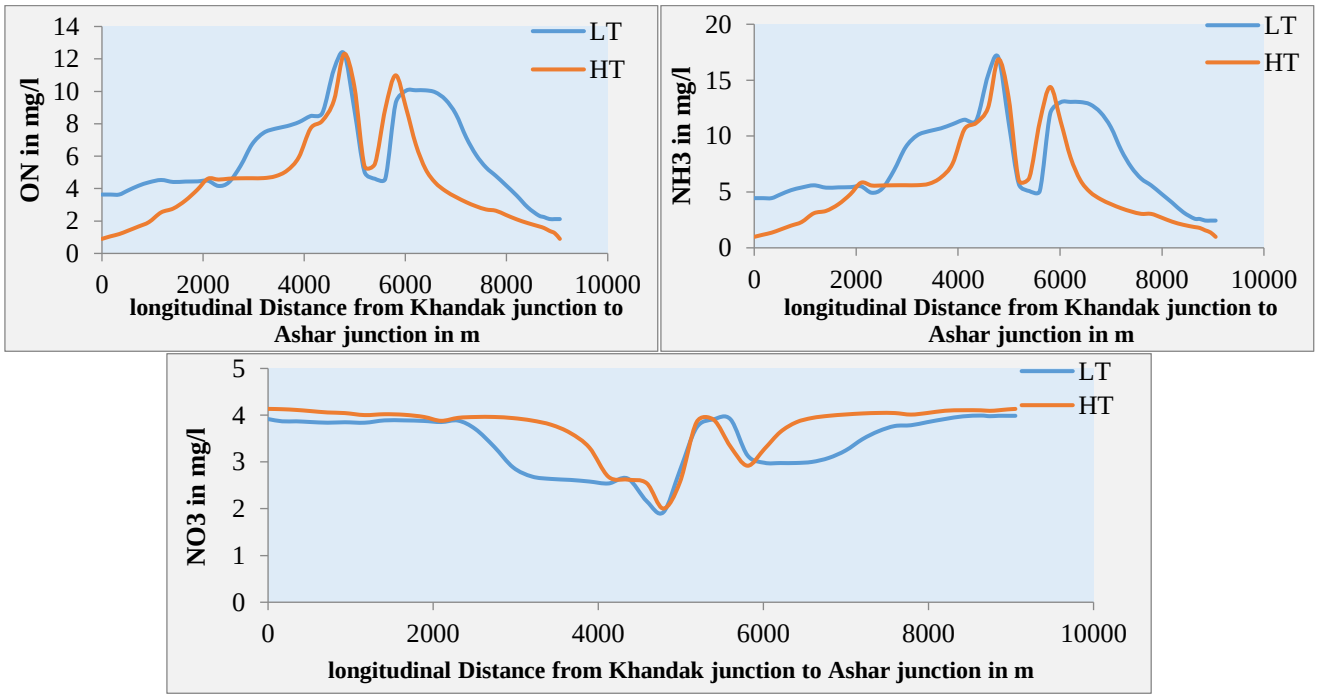


**Figure 17.** State variables of Nitrogen compound for KHandaq and Ashar Rivers

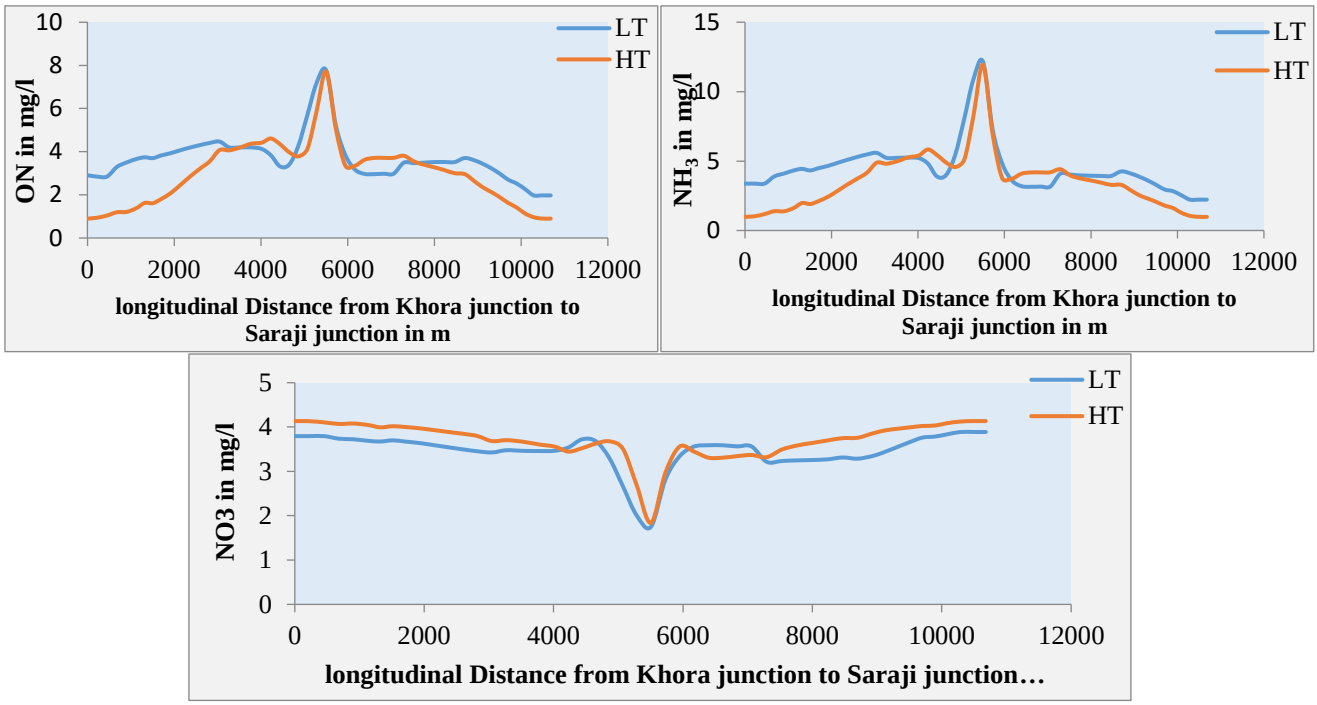


**Figure 18.** State variables of Nitrogen compound for Khora and Saraji Rivers

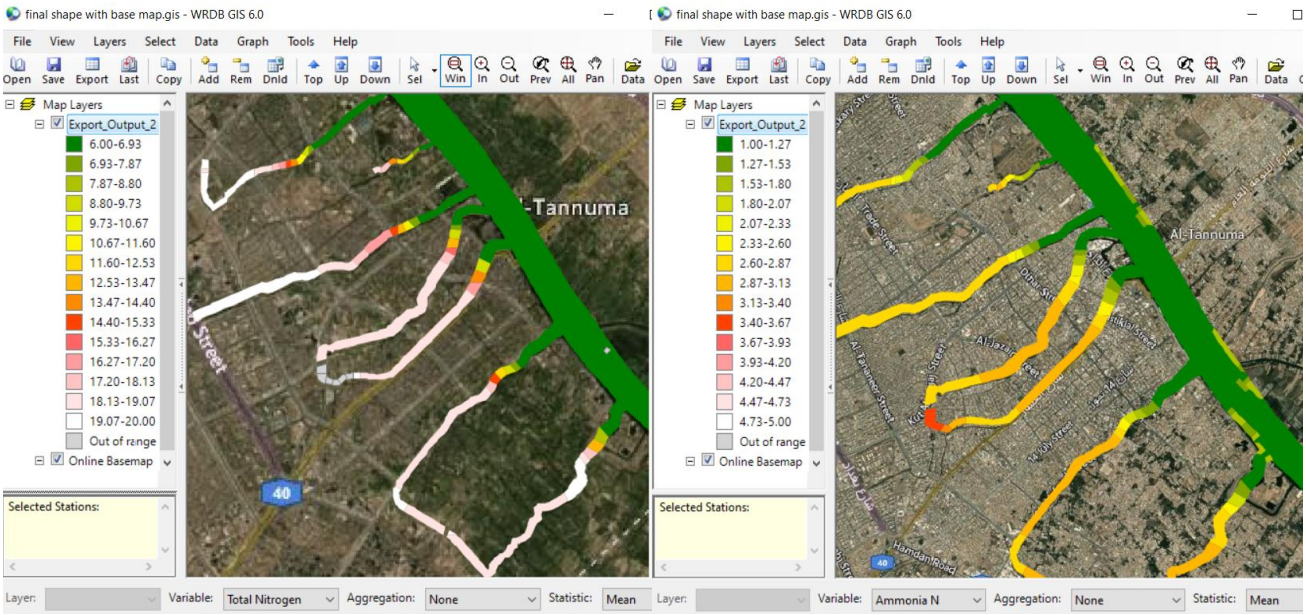


**Figure 19.** Spatial distribution of TN and $NH_3$ in Basrah Center

5.2.2 Phosphorus compounds state variables

OP and IP state variables are investigated and their results are plotted in Figure 20 (a) and Figure 20 (b) respectively. The figure tracked the results in consecutive periods, as fixed by legend, during the simulation time. In general, it was observed that there is a harmony between the results explaining the relationship between these compounds. For example, it has been observed that OP values decrease with time, while corresponding to an increase in IP values, in the mineralization process. The results varied from (0.5 to 0.45), and (0.3 to 0.34) mg/l at Basrah Center for OP, and IP respectively.

The corresponding results of these state variables of the main branches were shown in Figures 21-24. All results were calculated at two different periods, HT and LT according to the Basrah Center tide table. It can be concluded from these figures the following.

• During HT, the concentration of OP has been reduced because of the dilution process that occurs through interring additional water volume to the streams which in turn, increases mineralization process.

• During HT, the concentration of IP has been reduced because of the dilution process that occurs by interring additional water volume into the streams.

• The concentrations of phosphorus compounds state variables were slightly affected by the tide at the far ends of the Rivers from the Shatt Al Arab River because the flow velocity at these dead ends was approximately zero.

Colored spatial distributions of the TP are plotted in Figure 25. As shown in the figure, the main branches have high values compared with the river.

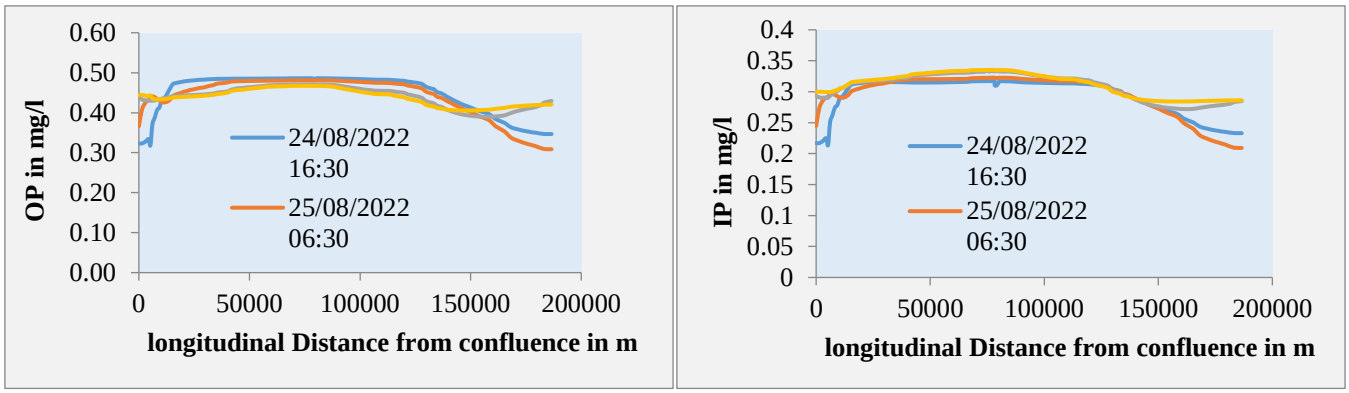


**Figure 20.** (a) OP variation along the Shatt Al Arab River at different periods; (b) IP variation along the Shatt Al Arab River at different periods

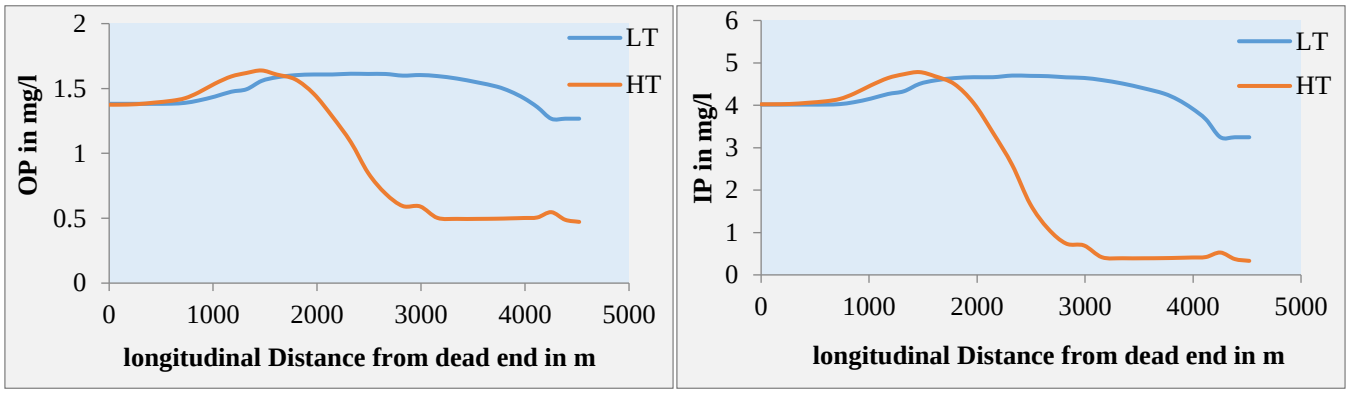


**Figure 21.** State variables of phosphorus compound for Jubyla River

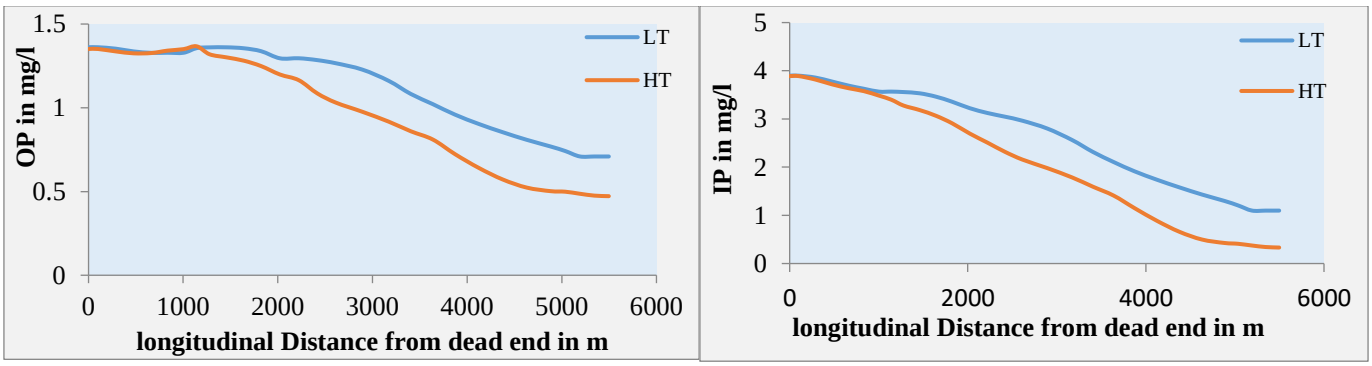


**Figure 22.** State variables of phosphorus compound for Robat River

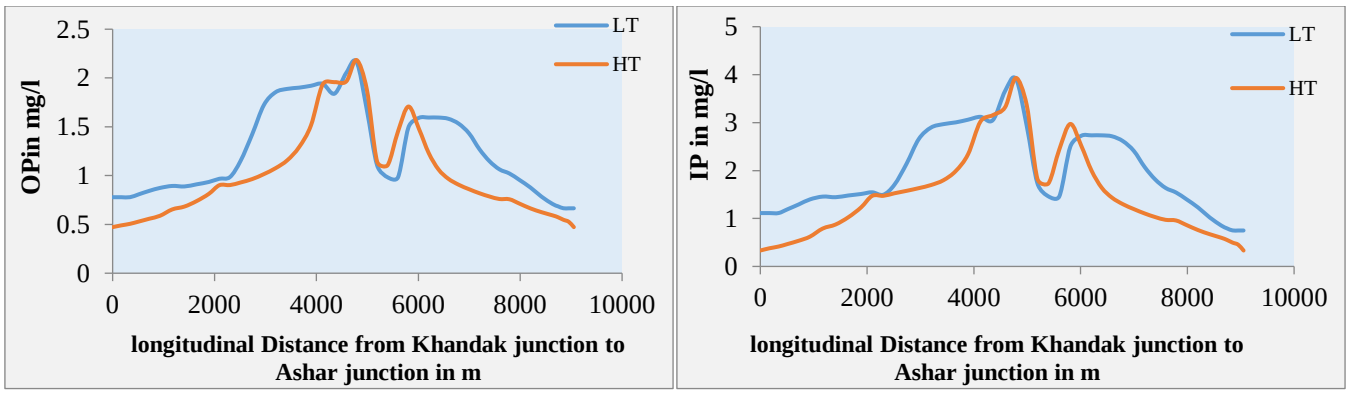


**Figure 23.** State variables of phosphorus compound for Khandaq and Ashar Rivers

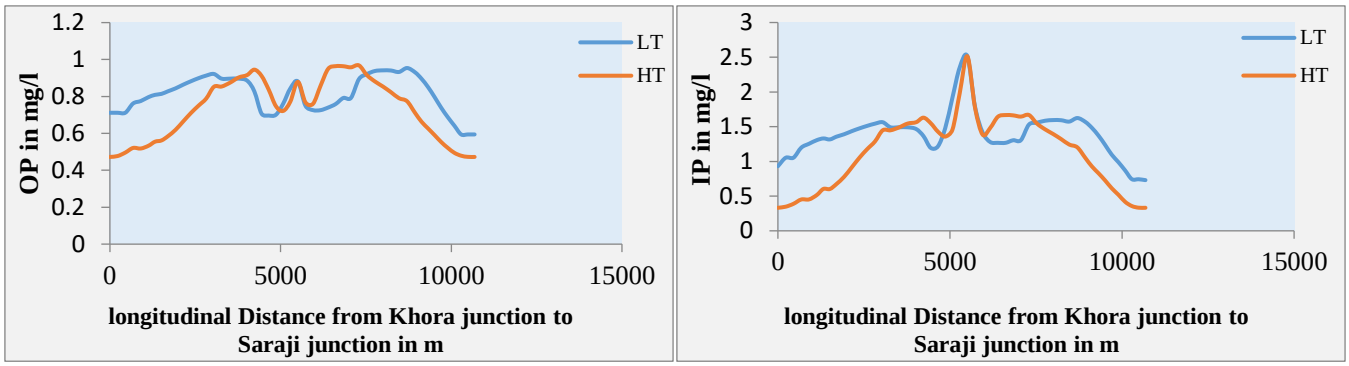


**Figure 24.** State variables of phosphorus compound for Khora and Saraji Rivers

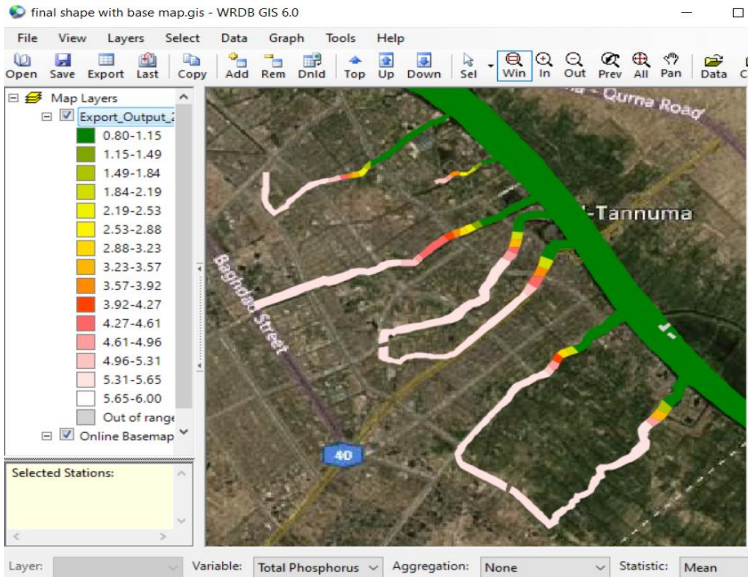


**Figure 25.** Spatial distribution of TP in Basrah Center

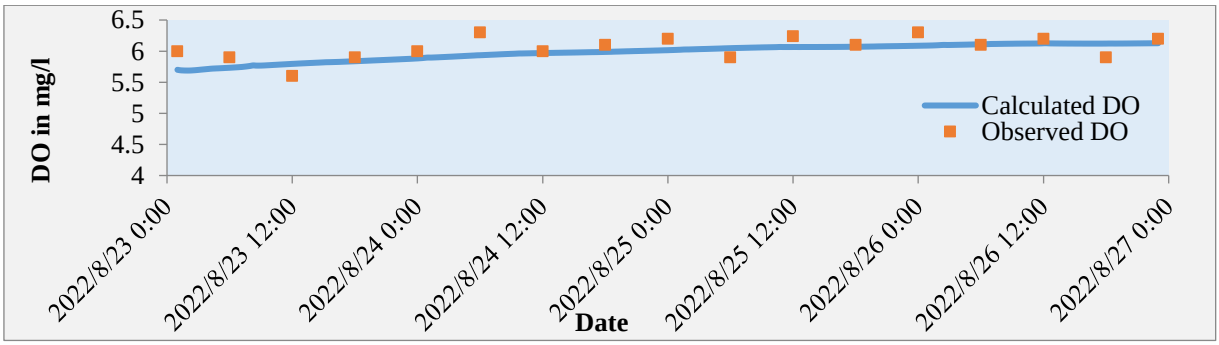


**Figure 26.** DO variation at Basrah Center station during simulation time

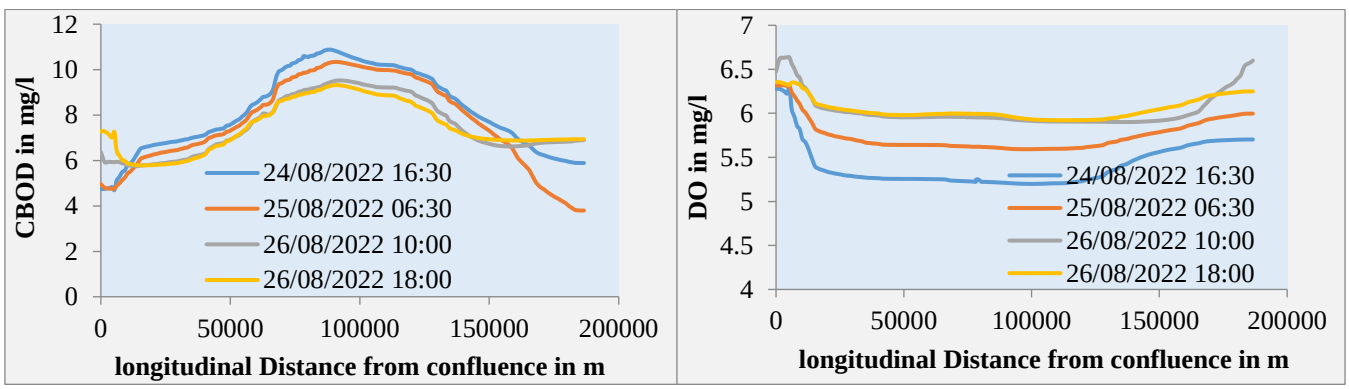


**Figure 27.** CBOD and DO distribution along the Shatt Al Arab River

5.2.3 CBOD and DO state variables

The state variables of CBOD and DO are considered, in detail, in the Shatt Al Arab River and it is branched. A validation step has been made during a comparison between the calculated and observed data of DO at Basrah Center through plotting time series graph as shown in Figure 26.

The longitudinal variations of the CBOD, DO along the River are studied and the results were plotted in Figure 27. The figure tracked the results in consecutive periods, as fixed by legend, during the simulation time. In general, it was observed that there is a harmony between the results explaining the relationship between these state variables. It has been observed that CBOD values decrease with time, while corresponding to an increase in DO values. This outcome can be attributed to the inverse relationship between the concentration of organic substances and bacterial activity in their oxidation process, leading to a corresponding decrease in oxygen consumption. The results varied from (11.0 to 9.0), and (5.2 to 6.0) mg/l at Basrah Center for CBOD and DO, respectively. Although CBOD values are decreasing, but they have large ranges at Basrah Center site compared with other sites because of the contribution of the point's sources of pollution that are located on main branches.

The corresponding results of these state variables of the main branches were shown in Figures 28-31. All results were calculated at two different periods, HT and LT according to Basrah Center tide table. It can be concluded from these figures the following.

• During HT, the concentration of CBOD has been reduced because of the dilution process that occurs through interring additional water volume into the streams.

• During HT, the concentration of DO has been increased because of the replenishment process that occurs through interring additional water volume into the streams during HT period.

• The concentration of CBOD and DO state variables were slightly affected by the tide at the far ends of the Rivers from the Shatt Al Arab River because the flow velocity at these dead ends was approximately zero.

• It has been noted that the DO values increased, while corresponding to a decrease in CBOD values.

A spatial distribution of DO and CBOD state variables at different locations of the study area are illustrated in Figure 32. The Figure 32 (a) showed the DO concentration in Basrah Center where the main branches appeared. Al the main branches have low value of DO, (2-3.5) mg/l, in far parts and (4.6-5.6) mg/l in parts near to the junction points. The river has value ranged (5.4-5.6) mg/l. the corresponding values of the CBOD concentration was (8-10) mg/l in the river while was (15-23) mg/l and (57-60) mg/l in near and far of the junction points respectively, see Figure 32 (b). the distribution of the DO and CBOD at Fao City was shown in Figure 32 (c) and Figure 32 (d) respectively.

5.2.4 PHYTO state variable

PHYTO state variable presented by chll-a is considered for the Shatt Al Arab River as well as the main branches. Where, this variable connects all other variables in the EUTRO model. Figure 33 shows the variation of PHYTO along the River at different times during the simulation period. As appeared from this figure, the concentration of PHYTO has a range of (5-25) g/l at 23000 m from Qurnah site, (1-4) g/l at Basrah Center site, and (14-35) g/l at 30000 m from Fao site. It is worth mentioning there are three levels of eutrophication according to the study [34].

1. Oligotrophic. Average Chl a concentration < 20 mg/m3,
2. Mesotrophic. Average Chl a concentration < 70 mg/ m3,
3. Eutrophic. Average Chl a concentration ⩾ 70 mg/ m3.

So, depending on this classification, Shatt Al Arab River has a Mesotrophic level in most its course.

The corresponding results of the PHYTO of the main branches were shown in Figure 34. The results were calculated at two different periods, HT and LT according to Basrah Center tide table. During HT, it can be concluded from the figure that the concentration of PHYTO has been reduced, for the streams part near the Shatt Al Arab River, because of the dilution process of nutrients that occur through interring additional water volume to the streams during HT period. While in streams part far away from the tide effect, the concentration of PHYTO was increased due to high concentrations of nutrients because of the point's course pollution.

The relationship between PHYTO and other state variables of EUTRO model has been observed and the results at the simulation end of PHYTO vs temperature, PHYTO vs DO, PHYTO vs NH3, and PHYTO vs IP are plotted in Figures 35-38 respectively. It can be concluded from these figures the following.

• The concentration of PHYTO has been increased or decreased directly proportional to the increasing or decreasing of water temperature. This is due to the increased activity of PHYTO with temperature rises and vice versa, see Figure 35.

• The concentration of DO has been increased or decreased inversely proportional to decreasing or increasing of PHYTO. This is due to the increased of DO consumption when the PHYTO is available in a high concentration and vice versa, see Figure 36.

• The concentration of NH3 has been increased or decreased inversely proportional to decreasing or increasing of PHYTO. This is due to the increased of NH3 consumption when the PHYTO is available in a high concentration and vice versa, see Figure 37.

• The concentration of IP has been increased or decreased inversely proportional to decreasing or increasing of PHYTO. This is due to the increased of IP consumption when the PHYTO is available in a high concentration and vice versa, see Figure 38.

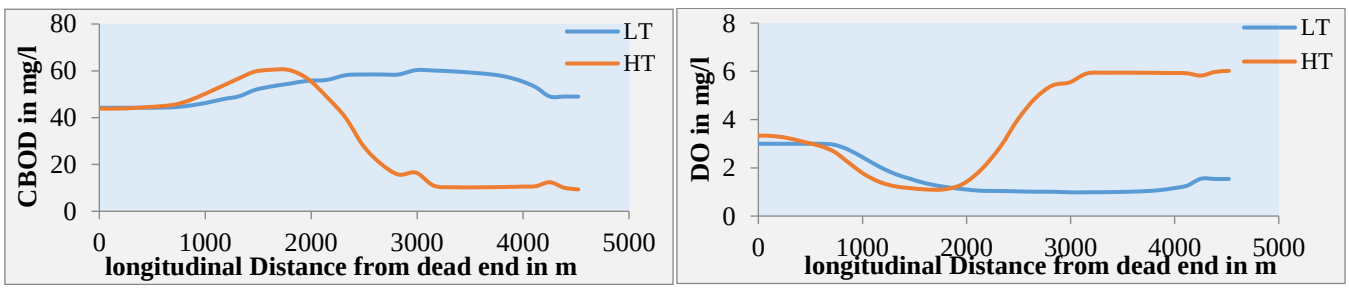


**Figure 28.** CBOD and DO distribution along the Jubyla River

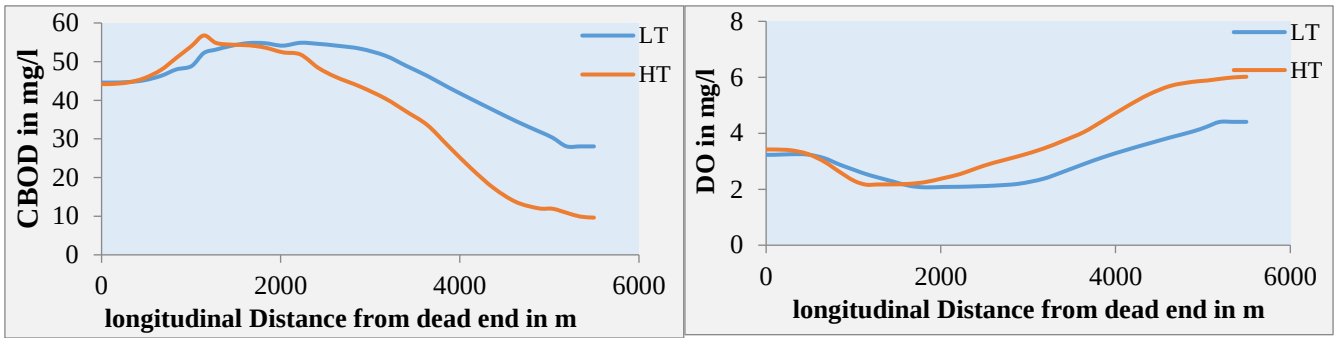


**Figure 29.** CBOD and DO distribution along the Robat River

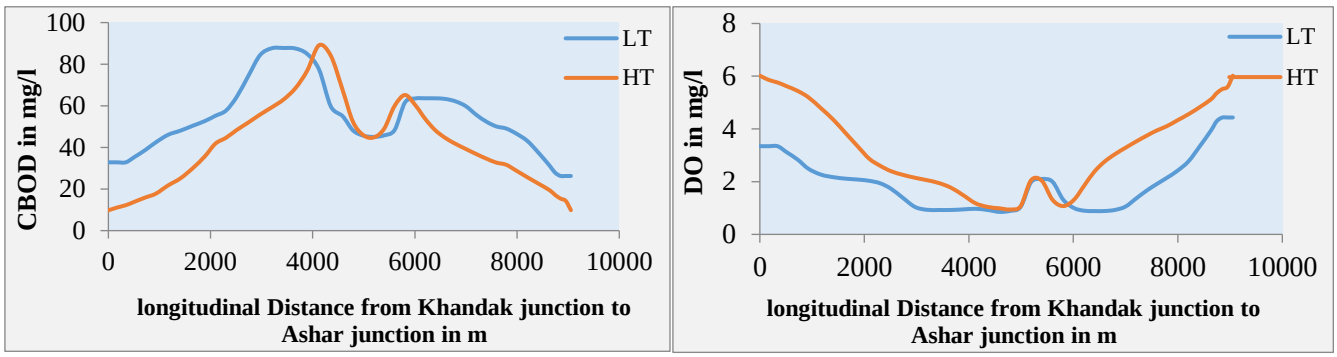


**Figure 30.** CBOD and DO distribution along the Khandaq and Ashar Rivers

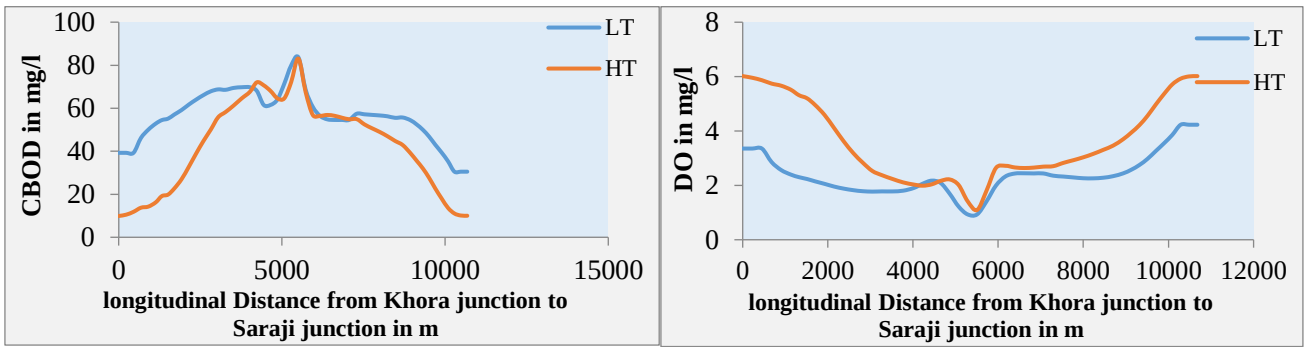


**Figure 31.** CBOD and DO distribution along the Khora and Saraji Rivers

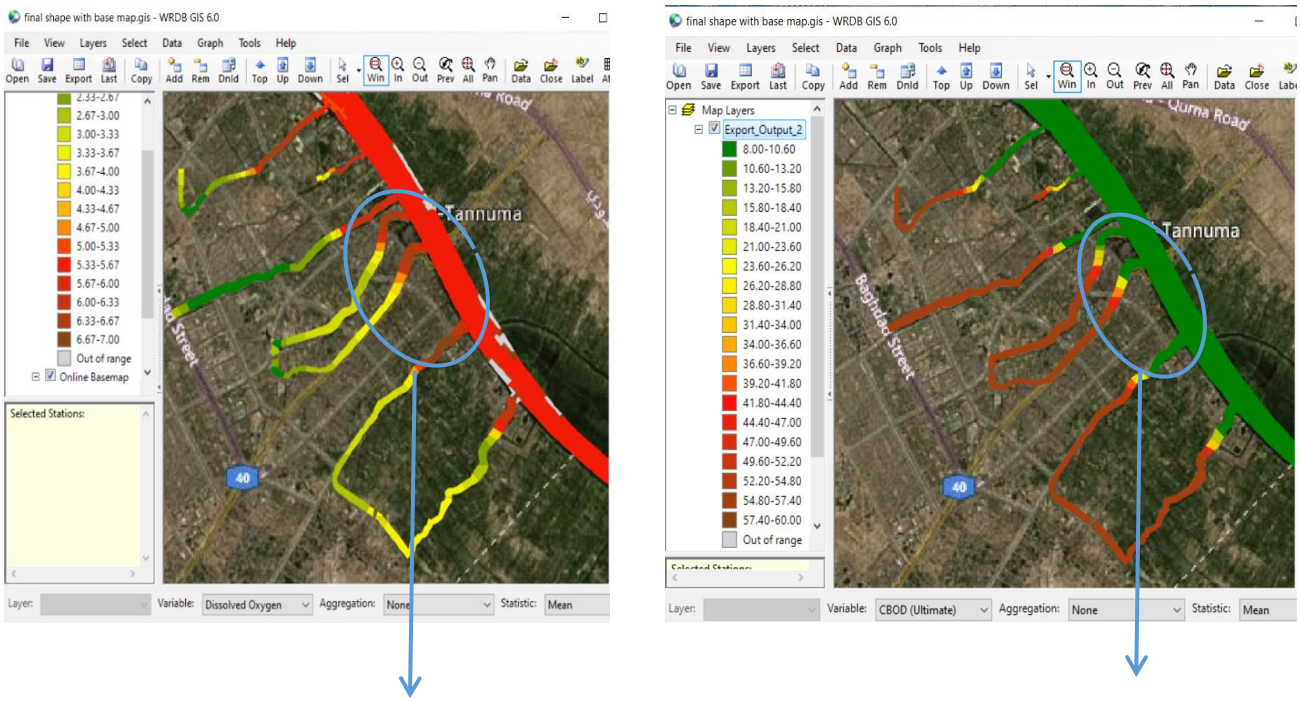

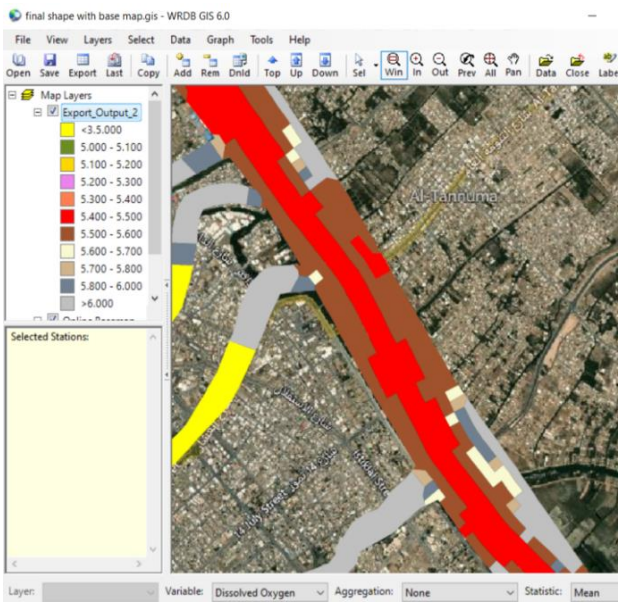


(a) DO in Basrah Center

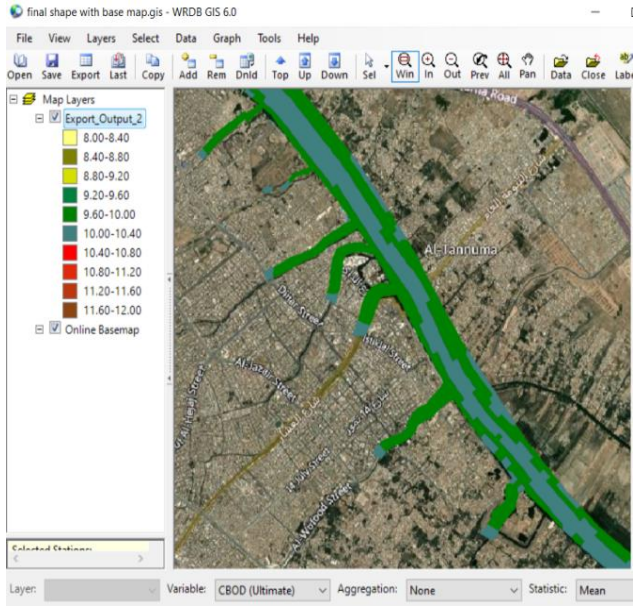


(b) CBOD in Basrah Center

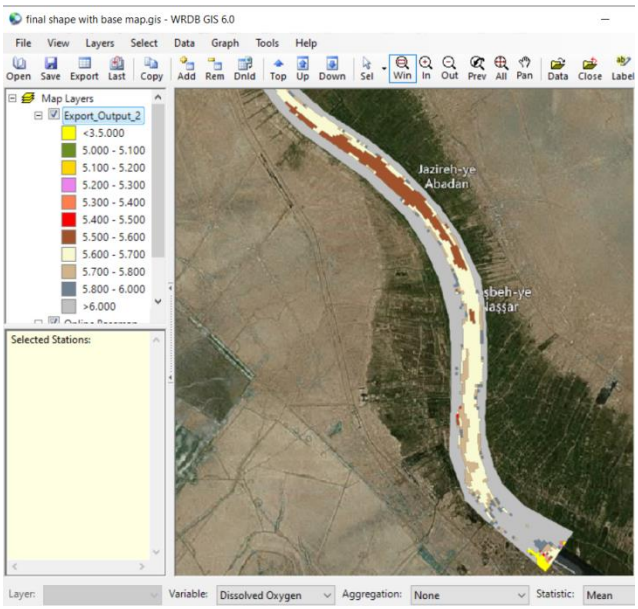


(c) DO in Fao City

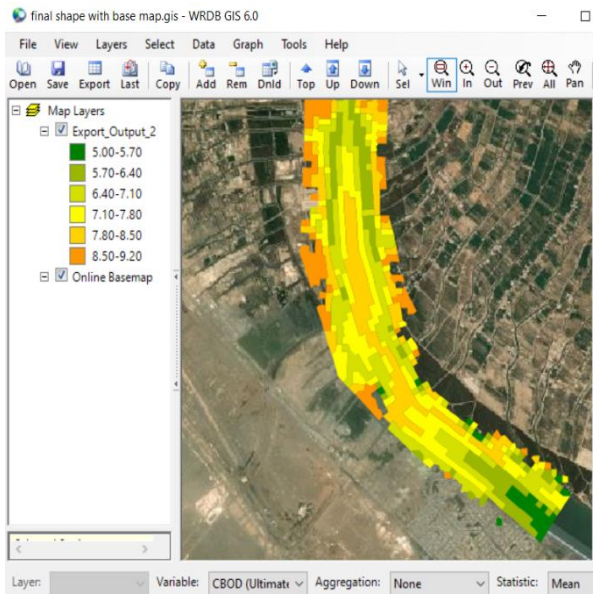


(d) CBOD in Fao City

**Figure 32.** A spatial distribution of the DO and CBOD state variables at different locations of the study area

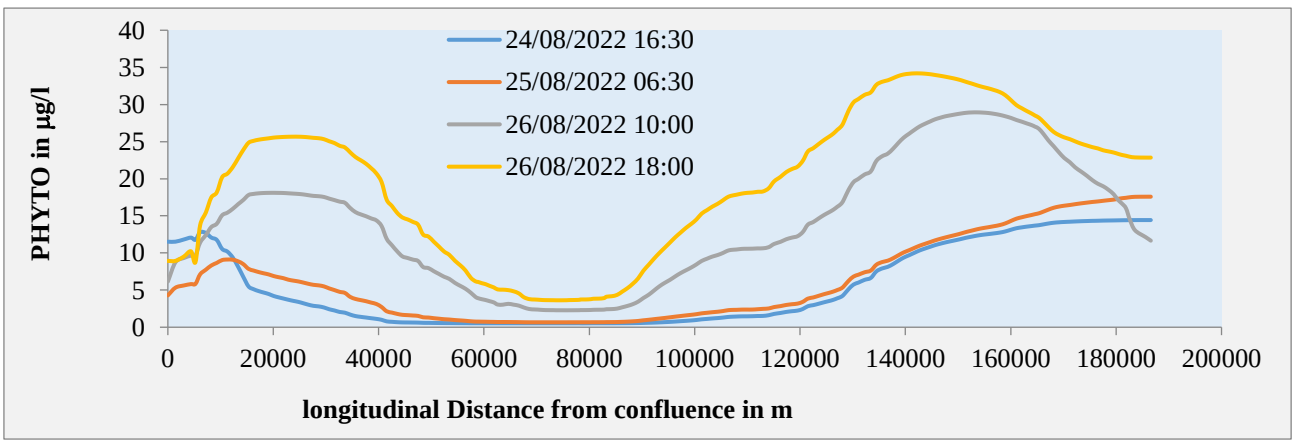


**Figure 33.** PHYTO distribution along the Shatt Al Arab River

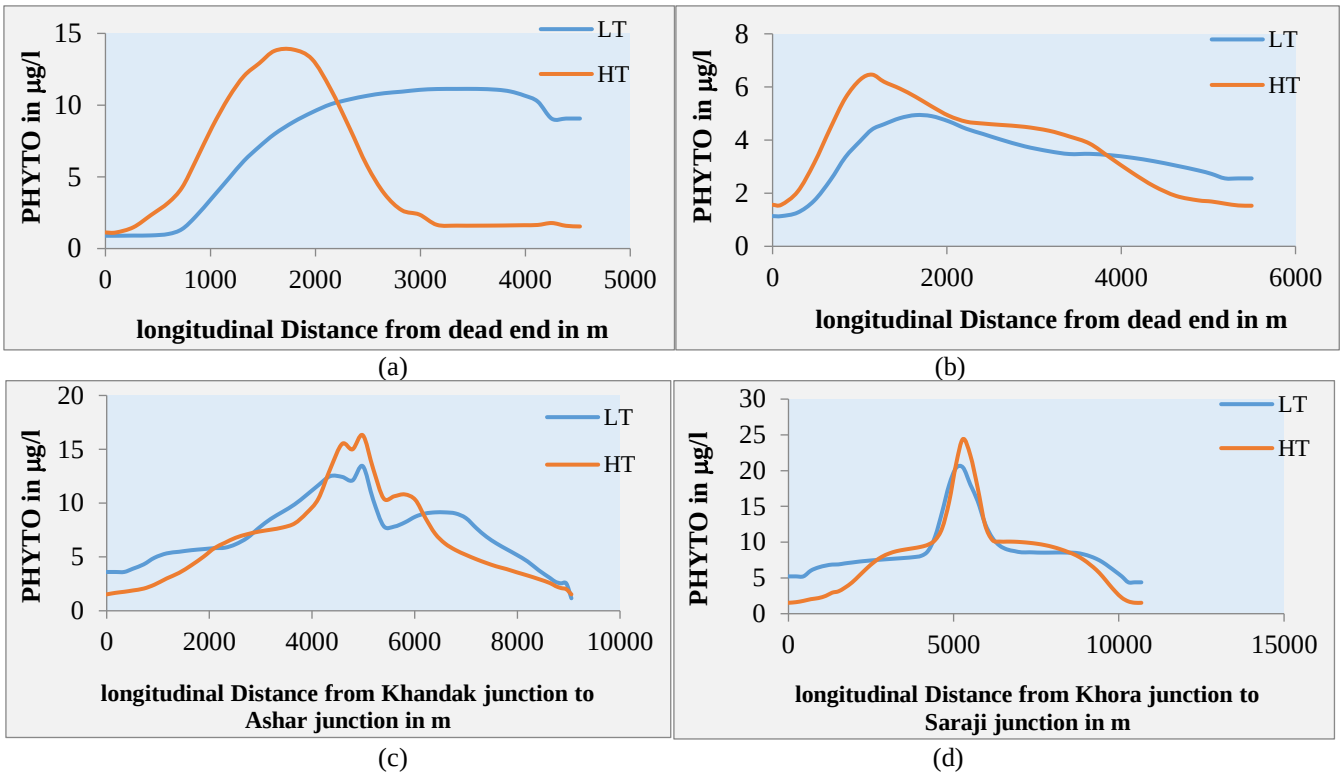


**Figure 34.** (a) PHYTO distribution along the Jubyla Rover; (b) PHYTO distribution along the Robat River; (c) PHYTO distribution along the Khandaq and Ashar Rivers; (d) PHYTO distribution along the Khora and Saraji Rivers

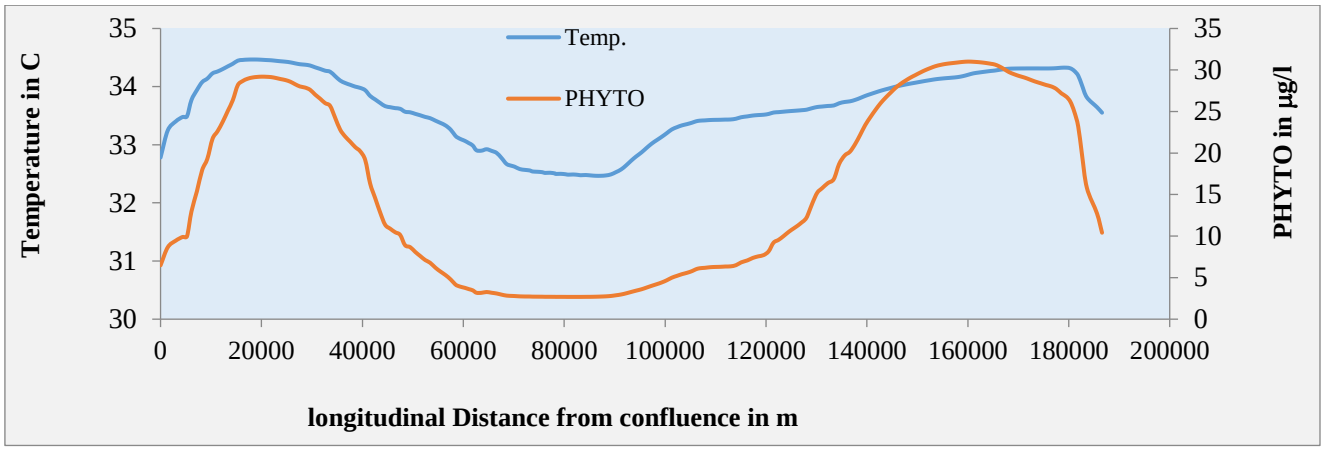


**Figure 35.** PHYTO vs water temperature distribution along the Shatt Al Arab River

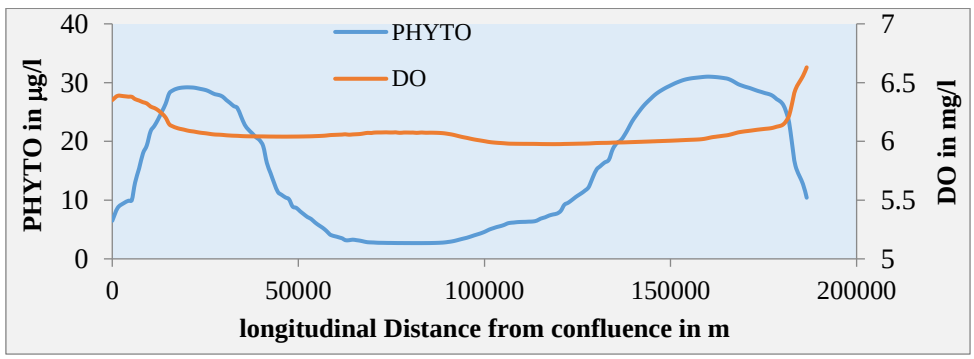


**Figure 36.** PHYTO vs DO distribution along the Shatt Al Arab River

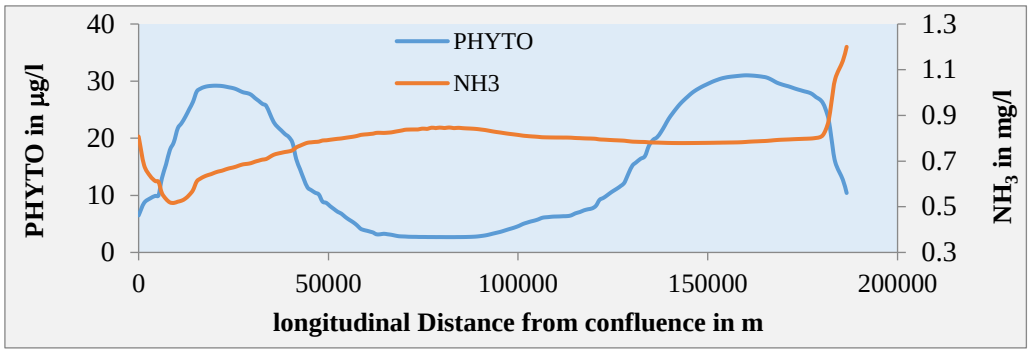


**Figure 37.** PHYTO vs $NH_3$ distribution along the Shatt Al Arab River

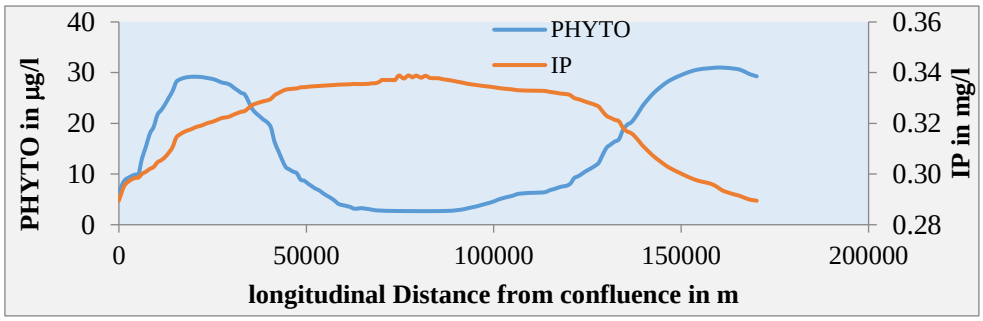


**Figure 38.** PHYTO vs IP distribution along the Shatt Al Arab River

## 6. CONCLUSION

Based on the results obtained, it can be observed that the concentrations of ON, $NH_3$, $NO_3$, OP, IP, and CBOD exhibit significant variations at the Basrah Centre site in comparison to the other sites. This can be attributed to the substantial influence of point sources of pollution situated along the main branches in the vicinity. Tidal phenomena exerted an influence on the concentrations of the state variables. During HT, ON, $NH_3$, OP, CBOD, and IP concentrations decrease due to dilution processes, increasing mineralization. phosphorus/nitrogen compounds, CBOD, and DO state variables are slightly affected by tide at far ends of rivers from Shatt Al Arab River due to zero flow velocity. The river water quality model combines the effect of its hydrodynamic characteristics and natural reaction mechanism on the law of mass conservation. The models are used to evaluate which alternative might be most effective in solving a water quality problem. So, from the building procedures and the applications, the following conclusions have been made.

Due to the inability of HEC-RAS software to deal with water quality modeling in the case of 2D simulation, three types of models have been considered to build the comprehensive Shatt Al Arab River model; hydrodynamic, temperature, and water quality models. The merge between 2D HEC-RAS and WASP water quality model framework has been used. The study area covers the entire course of the river from the confluence of the Tigris and Euphrates Rivers in Qurnah district to its mouth in Al Fao City, 10 km from Arabian Gulf. The river situation was unsteady and the influence of the tidal phenomenon was taken into consideration in the model-building, as well as the main River branches were taken into account which was overall the most important reason that made the simulation of the river complex. It was taken the effect of the main branches in the center of Basrah province which were the main source of the pollutant to the Shatt Al Arab River.

It is possible to develop this model in future studies to be able to model and study the Embedding the benthic layer within the water column of the river to represent the settling particulate matters and study their effect on the oxygen level by SOD and Including the macro algae state variable to study the conditions suitable for the spread of what is known as red tide (algal bloom).

## REFERENCES

[1] Zhao, E., Kuo, Y.M., Chen, N. (2021). Assessment of water quality under various environmental features using a site-specific weighting water quality index. Science of the Total Environment, 783: 146868. https://doi.org/10.1016/j.scitotenv.2021.146868

[2] Uddin, M.G., Nash, S., Olbert, A.I. (2021). A review of water quality index models and their use for assessing surface water quality. Ecological Indicators, 122: 107218. https://doi.org/10.1016/j.ecolind.2020.107218

[3] Uddin, M.G., Nash, S., Rahman, A., Olbert, A.I. (2022). A comprehensive method for improvement of water quality index (WQI) models for coastal water quality assessment. Water Research, 219: 118532. https://doi.org/10.1016/j.watres.2022.118532

[4] Yan, T., Shen, S.L., Zhou, A. (2022). Indices and models of surface water quality assessment: Review and perspectives. Environmental Pollution, 308: 119611. https://doi.org/10.1016/j.envpol.2022.119611

[5] Mawat, M., Hamdan, A.N. (2023). Review of mathematical surface water's hydrodynamic/water quality models with their application on the Shatt Al Arab River Southern Iraq. European Journal of Engineering Science and Technology, 6(1): 30-49.

https://doi.org/10.33422/ejest.v6i1.1057
[6] Datta, A.R., Kang, Q., Chen, B., Ye, X. (2018). Fate and transport modelling of emerging pollutants from watersheds to oceans: A review. Advances in Marine Biology, 81: 97-128. https://doi.org/10.1016/bs.amb.2018.09.002
[7] Liu, C.C., Lin, P., Xiao, H. (2021). Water Environment Modeling. CRC Press.
[8] Wool, T.A., Davie, S.R., Rodriguez, H.N. (2003). Development of three-dimensional hydrodynamic and water quality models to support total maximum daily load decision process for the Neuse River Estuary, North Carolina. Journal of Water Resources Planning and Management, 129(4): 295-306. https://doi.org/10.1061/(ASCE)0733-9496(2003)129:4(295)
[9] Ernst, M.R., Owens, J. (2009). Development and application of a WASP model on a large Texas reservoir to assess eutrophication control. Lake and Reservoir Management, 25(2): 136-148. https://doi.org/10.1080/07438140902821389
[10] Fan, C., Ko, C.H., Wang, W.S. (2009). An innovative modeling approach using Qual2K and HEC-RAS integration to assess the impact of tidal effect on River Water quality simulation. Journal of environmental management, 90(5): 1824-1832. https://doi.org/10.1016/j.jenvman.2008.11.011
[11] Quijano, J.C., Zhu, Z., Morales, V., Landry, B.J., Garcia, M.H. (2017). Three-dimensional model to capture the fate and transport of combined sewer overflow discharges: A case study in the Chicago Area Waterway System. Science of the Total Environment, 576: 362-373. https://doi.org/10.1016/j.scitotenv.2016.08.191
[12] Defne, Z., Spitz, F.J., DePaul, V., Wool, T.A. (2017). Toward a comprehensive water-quality modeling of Barnegat Bay: Development of ROMS to WASP coupler. Journal of Coastal Research, 78: 34-45. https://doi.org/10.2112/SI78-004.1
[13] Chueh, Y.Y., Fan, C., Huang, Y.Z. (2021). Copper concentration simulation in a river by SWAT-WASP integration and its application to assessing the impacts of climate change and various remediation strategies. Journal of Environmental Management, 279: 111613. https://doi.org/10.1016/j.jenvman.2020.111613
[14] Khudair, K.M., Eraibi, N.A. (2017). Environmental impact of RO units installation in main water treatment plants of Basrah city/south of Iraq. Desalination, 404: 270-279. https://doi.org/10.1016/j.desal.2016.11.020
[15] Hamdan, A.N.A., Al-Mahdi, A.A.J., Mahmood, A.B. (2020). Modeling the effect of sea water intrusion into Shatt Al-Arab River (Iraq). Journal of University of Babylon for Engineering Sciences, 28: 210-224.
[16] Mohammed, A.A., Al Chalabi, A.S. (2022). Environmental impact assessment study for Shatt Al-Arab River receiving industrial wastewater. Basrah Journal for Engineering Sciences, 22(1): 93-98. http://doi.org/10.33971/bjes.22.1.11
[17] Al-Asadi, S.A., Alhello, A.A., Ghalib, H.B., Muttashar, W.R., Al-Eydawi, H.T. (2023). Seawater intrusion into Shatt Al-Arab River, Northwest Arabian/Persian Gulf. Journal of Applied Water Engineering and Research, 11(2): 289-302. https://doi.org/10.1080/23249676.2022.2113460
[18] Naseh Ahmed, A., Dawood, A.S. (2016). Neural network modelling of TDS concentrations in Shatt Al-Arab River water. Engineering and Technology Journal, 34(2): 334-345. https://doi.org/10.30684/etj.34.2A.12
[19] Abd-El-Mooty, M., Kansoh, R., Abdulhadi, A. (2016). Challenges of water resources in Iraq. Hydrology Current Research, 7(4): 1-8. https://doi.org/10.4172/2157-7587.1000260
[20] Hamdan, A.N. (2016). Simulation of salinity intrusion from Arabian gulf to Shatt Al-Arab River. Basrah Journal for Engineering Science, 16(1): 28-32.
[21] Abdullah, A.D. (2017). Modelling Approaches to Understand Salinity Variations in a Highly Dynamic Tidal River: The Case of the Shatt Al-Arab River. CRC Press, USA.
[22] Kadhim, A.A. (2018). Measuring and modeling the effects of sea level rise on near-coastal riverine regions: A geospatial comparison of the Shatt Al-Arab River in Southern Iraq with the Mississippi River Delta in Southern Louisiana. Ph.D. dissertation. Michigan State University, USA. https://doi.org/doi:10.25335/aq17-qq73
[23] Hamdan, A., Dawood, A., Naeem, D. (2018). Assessment study of water quality index (WQI) for Shatt Al-arab River and its branches, Iraq. In MATEC Web of Conferences, 162: 05005. https://doi.org/10.1051/matecconf/201816205005
[24] Mohamed, A.R.M., Abood, A.N. (2017). Ecological health assessment of the Shatt Al-Arab River, Iraq. Environmental Science, 10(10): 1-8. http://dx.doi.org/10.9790/2380-1010010108
[25] Yaseen, B.R., Al Asaady, K.A., Kazem, A.A., Chaichan, M.T. (2016). Environmental impacts of salt tide in Shatt Al-Arab-Basra/Iraq. IOSR Journal of Environmental Science, Toxicology and Food Technology, 10(1-2): 35-43. https://doi.org/10.9790/2402-10123543
[26] Brunner, G.W. (2016). HEC-RAS River Analysis System: Hydraulic Reference Manual, Version 5.0. U.S. Army Corps of Engineers-Hydrologic Engineering Center, California, USA.
[27] Najm, A.T. (2017). Applications of two-dimensional surface flow modelling for Shatt Al-Arab River in civil engineering/water resources. University of Basrah.
[28] Orlob, G.T. (1983). Mathematical Modeling of Water Quality: Streams, Lakes and Reservoirs. John Wiley & Sons.
[29] Umgiesser, G., Ferrarin, C., Bajo, M., Bellafiore, D., Cucco, A., De Pascalis, F., Dhezzo, M., McKiver, W., Arpaia, L. (2022). Hydrodynamic modelling in marginal and coastal seas-The case of the Adriatic Sea as a permanent laboratory for numerical approach. Ocean Modelling, 179: 102123. https://doi.org/10.1016/j.ocemod.2022.102123
[30] Mawat, M.J., Hamdan, A.N.A. (2023). Simulation of 2D depth averaged Saint Venant model of Shatt Al Arab River south of Iraq. International Journal of Design & Nature and Ecodynamics, 18(3): 583-592. https://doi.org/10.18280/ijdne.180310
[31] Mawat, M.J., Hamdan, A.N.A. (2023). Integration of numerical models to simulate 2D hydrodynamic/water quality model of contaminant concentration in Shatt Al-Arab River with WRDB calibration tools. Open Engineering, 13(1): 20220416. https://doi.org/10.1515/eng-2022-0416

[32] Montgomery, H., Thom, N.S., Cockburn, A. (1964). Determination of dissolved oxygen by the Winkler method and the solubility of oxygen in pure water and sea water. Journal of Applied Chemistry, 14(7): 280-296. https://doi.org/10.1002/jctb.5010140704
[33] Al-waeli, A.A.A. (2021). Ecological and taxonomical study of the phytoplankton (non- diatoms) in the waters of the Shatt Al-Arab. College of Education for Pure Sciences Biology Department, Basrah University, Iraq.
[34] Ji, Z.G. (2017). Hydrodynamics and Water Quality: Modeling Rivers, Lakes, and Estuaries. John Wiley & Sons, Inc., New Jersey, USA. https://doi.org/10.1002/9781119371946